

Aus dem Institut für integrative Neuroanatomie
der Medizinischen Fakultät Charité – Universitätsmedizin Berlin

DISSERTATION

“Virtual Pre-embedding Labeling”:
A Method for Correlative Fluorescence and Electron
Microscopic Imaging and Double-Labeling in the Central
Nervous System of the Rat

zur Erlangung des akademischen Grades
Doctor medicinae (Dr. med.)

vorgelegt der Medizinischen Fakultät
Charité – Universitätsmedizin Berlin

von

Vince István Madai
aus Budapest

Gutachter: 1. Prof. Dr. R. W. Veh
 2. Prof. Dr. J. H. R. Lübke
 3. Ph.D. D. S. Zahm

Datum der Promotion: 03. Juni 2012

*Dedicated to my grandparents Katalin and István,
whose continuous commitment and efforts made it possible*

Abbreviations	4
1. Introduction	5
1.1. Immunocytochemical methods in electron microscopy	6
1.1.1. Post-embedding techniques	7
1.1.2. Pre-embedding techniques	9
1.2. The use of pre- and post-embedding for double and multiple labeling	10
1.3. Correlative fluorescence and electron microscopic imaging	11
1.4. Aim of research	12
2. Materials and Methods	17
2.1. Chemicals and their abbreviations	17
2.2. Antibodies and their abbreviations	19
2.3. Antibody sequences and visualization	20
2.4. Dot blot assays	20
2.5. Synthesis of hapten-tyramides	21
2.6. Purification of biotinyl-tyramide	22
2.7. ELISA assays	22
2.7.1. Determination of column fractions containing biotinyl-tyramide	22
2.7.2. Determination of the concentration of purified biotinyl-tyramide	23
2.7.3. ELISA model system for the visualization of hapten-tyramides	23
2.8. Immunocytochemistry	24
2.8.1. Perfusion fixation	24
2.8.2. Cryostat sections for light microscopy	25
2.8.3. Analysis of cryostat sections for light microscopy	26
2.8.4. Vibratome sections for virtual pre-embedding	26
2.8.5. Double labeled brain sections for virtual pre-embedding and correlative microscopy	27
2.8.6. Analysis of double labeling and correlation studies	27
2.8.7. Embedding in araldite	28
2.8.8. Preparation of semithin and ultrathin sections	28

2.8.9. Post-embedding immunocytochemistry on semithin sections	28
2.8.10. Staining of semithin sections	29
2.8.11. Post-embedding immunocytochemistry on ultrathin sections	29
2.8.12. Staining of ultrathin sections	30
2.8.13. Analysis of ultrathin sections	30
3. Results	31
3.1. Virtual pre-embedding with haptenylated antibodies	31
3.1.1. Biotinylated and digoxigenylated primary antibodies are not suited for virtual pre-embedding	31
3.1.2. A biotinylated secondary antibody provides a weak, but specific signal with virtual pre-embedding	33
3.2. Virtual pre-embedding with CARD	33
3.2.1. Purified hapten-tyramide conjugates have no benefit in comparison with unpurified conjugates	35
3.2.2. Synthesized biotinyl-tyramide is superior to purchased biotinyl-tyramide	35
3.2.3. CARD signal intensity in ELISA-assays is dependent on the hapten-tyramide concentration	36
3.2.4. CARD signal intensity in immunocytochemistry is also dependent the hapten-tyramide concentration	37
3.2.5. Peroxidase-conjugated streptavidin is not suited for virtual pre-embedding	38
3.2.6. Biotinyl-tyramide CARD provides a strong and highly specific signal with virtual pre-embedding	39
3.2.7. Digoxigenyl-tyramide and fluoresceine-tyramide CARD are equally suited for virtual pre-embedding	40
3.2.8. Virtual pre-embedding with tetramethylrhodamine-tyramide CARD is well suited for correlative microscopy and double labeling	44

4. Discussion	47
4.1. Sensitivity of virtual pre-embedding is determined by optimal deposition of haptens in the pre-embedding step	47
4.2. Single labeling with virtual pre-embedding offers considerable advantages over routinely used pre-embedding techniques	50
4.3. Double labeling with virtual pre-embedding offers considerable advantages over routinely used pre-embedding techniques	51
4.4. Virtual pre-embedding is an easy-to-use and inexpensive alternative for correlative microscopy studies	52
4.5. Virtual pre-embedding may provide a useful new tool for future immunocytochemical studies of the CNS	54
5. Conclusion	55
6. Summary	56
7. Zusammenfassung	58
8. References	60
9. Danksagung	66
10. Erklärung	67
11. Lebenslauf und Bibliographie	68

Abbreviations¹

ABC	Avidin-biotinylperoxidase complex
BT	Biotinyl-tyramide
CARD	Catalyzed reporter deposition
CLEM	Correlative light and electron microscopy
CNS	Central nervous system
DAB	Diaminobenzidine
DT	Digoxigenyl-tyramide
ELISA	Enzyme linked immunosorbent assay
EM	Electron microscopy
FT	Fluoresceine-tyramide
GAD67	Glutamic acid decarboxylase 67
HRP	Horseradish peroxidase
IGE	Immunogold-silver-enhancement technique
LM	Light microscopy
QD	Quantum dot
SA	Streptavidin
TMRT	Tetramethylrhodamine-tyramide
TT	Texas-Red-tyramide
UV	Ultraviolet
VirP	Virtual pre-embedding

¹ Abbreviations of chemicals found in the materials and methods section are listed in paragraph 2.1. Abbreviations of antibodies are listed in paragraph 2.2

1 Introduction

Immunocytochemical techniques combine morphological, immunological and chemical methods to identify the cellular localization of antigens in cells and tissues. These techniques are widely used for both light (LM) and electron microscopy (EM).² EM, however, offers a considerably higher resolution than LM. In biological tissue sections, EM achieves a resolution of approximately 0.2 nm, compared to roughly 0.2 μm , when using LM. Owing to the superior resolution, immunolabeling for EM allows for the correlation of the immunosignal with the ultrastructure of cells and tissues by visualizing the exact morphology of subcellular structures and organelles. Thus, a precise localization of the target molecules is achieved³. In addition to localizing antigens, it is important in neuroscience to unequivocally identify the synaptic connections between cell types of different brain areas. For this purpose, tracing experiments are combined with double (or multi) immunolabeling techniques.

Immunolabeling techniques for both LM and EM offer particular advantages, however, a synergistic approach may be necessary in the field of neuroscience dealing with very complex types of tissue. One synergistic method is the correlation of fluorescence and electron microscopy allowing for the pre-examination of labeled cells or processes by screening the fluorescence signal in a comparatively large section. Regions of interest can then be chosen and further analyzed on the ultrastructural level by the use of EM.

Among other approaches in EM-immunocytochemistry, the use of so called haptens offers a stable affinity system for labeling.⁴ Haptens are small and chemically rather inert molecules, which by definition cannot elicit an immunological response on their own. Some haptens like biotin, tetramethylrhodamine and fluoresceine have been widely used in light microscopic immunocytochemistry.⁵

The aim of this thesis was to investigate the use of different haptens for immunocytochemical labeling in central nervous tissue sections in a combination of the two, generally different,

² (Asan, E et al. 2008)

³ (Afzelius, BA et al. 2004)

⁴ (Bratthauer, GL 1999)

⁵ (Chevalier, J et al. 1997; Bayani, J et al. 2004)

labeling techniques for electron microscopy, so called pre- and post- embedding labeling. This approach, termed virtual pre-embedding (VirP) in the present work, is a new immunocytochemical method, which offers considerable advantages over routinely used pre-embedding methods and is suited for above described correlative imaging and double labeling studies of the central nervous system (CNS).

1.1 Immunocytochemical methods in electron microscopy

A prerequisite for successful immunocytochemical labeling is fixation of the molecular constituents of cells and extracellular matrix in situ. Ideally, the method of choice to achieve this goal would be rapid freezing of the specimen⁶. However, chemical fixation is still commonly used, both in LM and EM⁷. Especially the investigation of complex and inhomogeneous tissues like brain tissue often strongly depends on the preservation of orientation, thus favoring chemical fixation as the method of choice. This is achieved by use of chemicals such as aldehydes.⁸ They rapidly crosslink a large variety of biomolecules in situ through their amino-groups, provided that diffusion distances are minimized by perfusion fixation. In EM, post-fixation with osmium tetroxide as a lipid fixative is a common technique.⁹ Osmium tetroxide crosslinks fatty acids leading to the stabilization of lipids against the effects of solvent treatment during dehydration and embedding. Thereby, preservation of membranes for ultrastructural analysis is improved.

Subsequent preparation steps are required for stabilization of the specimen for thin sectioning. This is achieved by embedding in artificial resins. Two structurally different types of resins are commonly used, namely epoxy and methacrylate resins.¹⁰ In contrast to the classical epoxy resins, which are polymerized in the heat, several types of acrylic resins were designed for both, high and low temperature embedding. It should be mentioned that loss of antigenicity, i.e. epitopes, occurs to different degrees with all types of resins used for embedding.

⁶ (McDonald, KL et al. 2006)

⁷ (Webster, P et al. 2008)

⁸ (Griffiths, G et al. 1993, p. 29ff)

⁹ (Raimondo, S et al. 2009)

¹⁰ (Newman, GR et al. 1999)

When compared to LM, embedding and interaction with the electron beam in EM require adaptive strategies for immunocytochemical labeling and visualization techniques. In ultrathin sections (30-100 nm) prepared from resin-embedded biological specimens, usually contrasting agents, i.e. heavy metal ions, are necessary to reveal structural details. The distinct affinity of subcellular structures to the heavy metal staining results in gray scale images. This implies that immunocytochemical markers have to be selected with respect to their "electron density", i.e. the ability to scatter electrons at large angles and to therefore appear relatively darker than the underlying tissue components. For immunocytochemistry, two generally different labeling approaches have been introduced. They differ with respect to labeling and visualization, being performed either prior to (pre-embedding techniques) or after (post-embedding techniques) the embedding step (Figure 1).

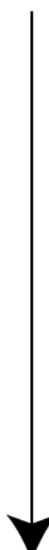
t	Pre-embedding method	Post-embedding method
	Fixation	Fixation
	Permeabilization	
	Immunolabeling	
	Visualization	
	Embedding	Embedding
		Immunolabeling
		Visualization
	EM analysis	EM analysis

Figure 1: Basic concepts of pre- and post-embedding labeling techniques. Whereas in pre-embedding methods antigens are labeled and visualized *prior to embedding*, in post-embedding techniques antigens exposed *after embedding* on the surface of tissue sections are labeled and visualized.

1.1.1 Post-embedding techniques

Post-embedding techniques rely on the fact that a subset of epitopes is still available for antibody binding at the surface of sections after the embedding step. When comparing epoxy and methacrylate resins, post-embedding labeling on epoxy-sections is clearly less frequently used. Apparently, on epoxy-sections only a comparatively small fraction of epitopes can be

successfully detected. This may be due to the fact that epoxy-resins covalently interact with a range of biomolecules, which could account for a significant decrease in the preservation of antigenicity of the target molecules.¹¹ Furthermore, epoxy-resins are highly hydrophobic and require a complete dehydration of the tissue with possible antigen denaturation prior to resin infiltration. In addition, epoxy resins require polymerization at temperatures above 50° Celsius, which constitutes another possible deteriorating effect on antigenicity.

Therefore, methacrylate resins like Lowicryl and LR type resins are widely used for post-embedding labeling, allowing labeling of peptide and protein antigens more frequently than epoxy-resins.¹² This may result from the unique biophysical properties of methacrylate resins. They tolerate small amounts of water, hence the specimen must not necessarily be completely dehydrated. Their low viscosity allows for low temperature dehydration and embedding, reducing deleterious solvent effects. (However, the extent to which a given antigen will be affected by different types of dehydrating solvents still cannot be predicted with certainty¹³). Moreover, methacrylates interact much less covalently with tissue constituents than epoxy resins. This is explained by the formation of submicroscopic cracks during sectioning exposing a higher number of antigens at the surface of the section, thus improving immunocytochemical labeling.¹⁴ Finally, some of these resins maintain a near water-like viscosity even at temperatures between -20 and -80 degrees Celsius. At these low temperatures, ultrastructural damage due to dehydration and an impairment of antigenicity seems less likely when compared to room temperature processing.

Colloidal gold particles are widely used as markers for post-embedding immunocytochemistry. Due to their high electron density, they offer excellent contrast even on heavy metal stained tissue sections. A large range of particle sizes is available. Usually, colloidal gold particles are coupled to secondary antibodies or protein A, a bacterial protein binding to the Fc-fragment of antibodies. Combined use of methacrylate resin embedding with colloidal gold labeling can be regarded as the standard method for post-embedding immunocytochemistry.¹⁵ It should be noted, however, that fine structure in methacrylate sections, at least after immunolabeling, tends to be less well preserved when compared to epoxy-resins, partly because membranes are not stabilized

¹¹ (Causton, BE 1986)

¹² (Shida, H et al. 1990)

¹³ (Carlemalm, E et al. 1982)

¹⁴ (Causton, BE 1986)

¹⁵ (Roth, J 1996; Stierhof, YD et al. 1986; Brorson, SH et al. 1994)

by osmium-tetroxide: As the relevant resins are usually polymerized with UV-light, osmication of the tissue prior to embedding has to be omitted¹⁶, as it would interfere with polymerization.

Despite all efforts, even with methacrylate embedding many antigens cannot be successfully detected with post-embedding methods.

1.1.2 Pre-embedding techniques

Generally, pre-embedding labeling techniques for EM are very similar to standard immunocytochemical methods used for LM. Permeabilization achieved by detergent treatment or freeze-thaw protocols is indispensable in either case, though more gently applied for EM to minimize ultrastructural damage.¹⁷ After permeabilization, antibodies will be able to penetrate several micrometers into cells or tissue sections, and bind to their respective antigen. Different approaches may then be used for visualization of bound antibodies. Osmication and embedding are carried out in a manner similar to standard morphological techniques. For embedding, epoxy-resins are used, given their already mentioned advantages regarding fine structural preservation when compared to methacrylates.

For visualization, two techniques became particularly popular in EM-based research. First, enzymatic labeling with horseradish peroxidase (HRP), to which a chromogen is presented as a substrate. This chromogen is then oxidized in the presence of hydrogen peroxide. Diaminobenzidine (DAB) as a chromogen was introduced to electron microscopy in 1966¹⁸ and has been widely used since then. The water-soluble DAB becomes insoluble by oxidation and forms a stable complex of brown color in the light microscope. The complex is osmiophilic and can therefore be identified as a dense precipitate with the electron microscope.

The second widely used technique is immunogold-silver-enhancement (IGE)¹⁹, based on the physical property of gold particles to induce the formation of a shell of elemental silver when exposed to silver salt in the presence of a reducing agent. For this purpose, small gold particles

¹⁶ (Carlemalm, E et al. 1982)

¹⁷ (Humbel, BM et al. 1998)

¹⁸ (Graham, RC, Jr. et al. 1966)

¹⁹ (Baschong, W et al. 1998)

(1-5 nm) are used in order to ensure a successful penetration of the gold conjugate.²⁰ The size of generated silver particles can be adapted and is usually between 20 and 200 nm. Owing to their size and electron density, they are easily identified with the electron microscope.

1.2 The use of pre- and post-embedding for double and multiple labeling

Both pre- and post-embedding techniques have been used to study the ultrastructure of the CNS. To identify the location of neuronal antigens at the EM level with a resolution of approximately 20 nm, post-embedding techniques, if applicable, would be preferred. Consequently, double or multiple post-embedding labeling permits localization of different antigens in the same or adjacent structures providing additional information regarding fine-structural co-localization and emerging functional implications.²¹ Strategies for post-embedding multiple labeling include application of different sizes of gold colloids or the combination of gold colloids with other available particulate markers like ferritin.²² Another option is to label different antigens on adjacent sections.

Pre-embedding techniques on the other hand are preferred for the study of CNS connectivity.²³ Combined with tracing studies, not only the connections, but also the neurotransmitters involved can be revealed. Double or multiple pre-embedding labeling also provides an adequate alternative to demonstrate co-localization of target molecules, when at least one of the antigens cannot be visualized by post-embedding methods. Individual pre-embedding multiple labeling strategies include combinations of DAB with autoradiography²⁴, DAB with other types of benzidines²⁵ and the combination of DAB with silver intensified gold particles²⁶.

²⁰ (Lackie, PM et al. 1985; Hainfeld, JF et al. 1992; Dulhunty, AF et al. 1993)

²¹ (Zini, N et al. 2004)

²² (Roth, J et al. 1978)

²³ (Griffiths, G et al. 1993, p. 363ff)

²⁴ (Silverman, AJ et al. 1983; Pickel, VM et al. 1986)

²⁵ (Lakos, S et al. 1986; Levey, AI et al. 1986; Norgren, RB, Jr. et al. 1989)

²⁶ (van den Pol, AN 1985)

1.3 Correlative fluorescence and electron microscopic imaging (CLEM)

Since the highly complex CNS tissue is composed of many different cell types and a delicate network of cellular processes, visualization techniques for demonstration of cellular and subcellular cell constituents have to surmount this complexity.²⁷ To this end, fluorescence microscopy proved to be a very useful tool allowing for the visualization of protein co-localization, interaction, dynamics and function.²⁸ However, in fluorescence microscopy resolution is limited not allowing fine structural analysis of labeled structures.²⁹ Electron microscopy, by contrast, though clearly offering this resolution, is restricted with respect to specimen dimensions, i.e. a grid size of roughly 3 mm. Furthermore, rare antigens may be difficult to trace within the area of a section. Hence, combination of fluorescence microscopy with subsequent electron microscopic analysis may overcome these limitations and allow for the examination of the same cells or processes on a range from large overviews to the nanometer scale.³⁰

For correlative microscopy, labeling has to be performed prior to embedding and is therefore restricted to pre-embedding methods. So far, several approaches have been introduced to correlate fluorescence with electron microscopy. The affinity system, e.g. an antibody, can be conjugated with both a fluorescence dye and ultrasmall gold (FluoroNanogold), so that after light microscopic evaluation a silver-enhancement procedure can be performed and the same labeling analyzed by electron microscopy.³¹ Another method called photoconversion is based on illuminating fluorescence labeled samples with strong UV-light to oxidize diaminobenzidine at the site of the fluorescence label, thus producing the stable and osmiophilic polymer known from the HRP-DAB system.³² The already analyzed fluorescence signal is thereby converted into a signal readily visible with the electron microscope. The method is applicable for a large variety of fluorescent dyes.³³ It also can be used in combination with epitope-tagging methods, such as the biarsenical-tetracysteine system, in which a genetically encoded tag binds to a precursor-

²⁷ (Heupel, WM et al. 2009)

²⁸ (Giepmans, BN 2008)

²⁹ (Mironov, AA et al. 2009)

³⁰ (Giepmans, BN 2008)

³¹ (Robinson, JM et al. 1997; Takizawa, T et al. 1998; Robinson, JM et al. 2000)

³² (Meiblitzer-Ruppitsch, C et al. 2008)

³³ (Lubke, J 1993)

form of fluoresceine, which becomes fluorescent upon binding.³⁴ Quantum dot nanocrystals (QDs)³⁵ are also in use for correlative microscopy. They consist of a cadmium-selenide (CdSe) or cadmium-telluride (CdTe) crystal core, surrounded by a zinc sulfide shell and an organic polymer coating. QDs provide a bright fluorescent signal with a long lifetime and distinct emission wavelengths, depending on their size.³⁶ Owing to their physical properties, they are moderately electron dense and can be identified according to their size and shape, thus permitting correlative imaging and multilabeling studies.³⁷ It is even possible to identify QDs with the help of energy filtering transmission electron microscopy (EFTEM) using cadmium specific energy loss.³⁸

1.4 Aim of Research

As discussed above, pre-embedding labeling techniques are necessary for the detection of rare antigens, for tracing studies and synergistic correlative microscopy approaches. However, the use of the existing main pre-embedding techniques, i.e. the immunoperoxidase (IP) method and the immunogold-silver-enhancement (IGE) method, is limited in practice. IP offers high sensitivity due the enzymatic nature of the reaction, but is limited by low resolution and obscuration of ultrastructural detail as a result of accumulation and diffusion of the reaction product. IGE on the other hand allows for precise localization, but is less sensitive than IP and standardization of the procedure is difficult. Moreover, the combination of existing pre-embedding methods is difficult. Therefore, alternative pre-embedding techniques are required, which are easy to use, suited for correlative approaches and double-labeling and which provide reproducible results, good contrast and high sensitivity.

In this context, one major focus in the development of immunocytochemical techniques was the improvement of sensitivity. For this purpose, an efficient method is the amplification of the signal by use of haptens. Haptens are small molecules, which by definition cannot elicit an immunological response, unless coupled to a carrier molecule. Some haptens are fluorochromes,

³⁴ (Griffin, BA et al. 1998; Martin, BR et al. 2005)

³⁵ (Bruchez, M, Jr. et al. 1998; Chan, WC et al. 1998)

³⁶ (Michalet, X et al. 2005)

³⁷ (Giepmans, BN et al. 2005)

³⁸ (Nisman, R et al. 2004)

making them ideal candidates for immunocytochemical methods. In 1989 Bobrow and colleagues introduced a new amplification system for immunocytochemistry based on the deposition of hapten-tyramides by a peroxidase reaction, called CARD (**C**Alyzed **R**eporter **D**eposition) or TSA (**T**yramide **S**ignal **A**mplification).³⁹ The amino acid tyramine serves as a substrate for the peroxidase and is oxidized in the presence of hydrogen peroxide leading to the formation of tyramine-radicals. These radicals have a short half-life and rapidly and covalently react with amino acids of nearby proteins. When coupled to a hapten, the hapten-tyramide is still recognized as a substrate with resulting deposition of large amounts of haptentylated tyramide in the vicinity of the antigen. Deposited hapten can be visualized in a consecutive step, either using secondary antibodies, the avidin/biotin system, or by direct hapten fluorescence, e.g. with tetramethylrhodamine or fluoresceine (Figure 2). The CARD technique enhances the signal about 8 to 10,000-fold, depending on the type of assay and the hapten-tyramide used.⁴⁰ CARD has been used in a large variety of immunocytochemical adaptations⁴¹, since many different hapten-tyramides are not only commercially available, but can also be synthesized relatively easily and at low costs.⁴² In fluorescence microscopy, either deposited biotin is labeled with a fluorophore-linked avidin⁴³ or the fluorescence signal of a hapten is visualized directly.⁴⁴ Fluorescence-CARD can also be combined with a directly fluorophore-labeled antibody for double-labeling studies.⁴⁵ The use of haptens is also interesting for electron-microscopic pre-embedding techniques. Due to the amplification step especially visualization of rare antigens is improved by CARD. Tyramine-conjugates have been used to intensify IP and IGE labeling and the DAB⁴⁶ or colloidal gold⁴⁷ signal. Even biotin-tyramide itself was used as a visualization-system producing a densely stained filamentous material.⁴⁸ All these approaches demonstrate that the CARD technique is well suited for amplification of an immunocytochemical signal due to the enzymatic nature of hapten deposition. Although sensitivity was much improved by

³⁹ (Bobrow, MN et al. 1989)

⁴⁰ (Bobrow, MN et al. 1991; Adams, JC 1992; Merz, H et al. 1995; Hunyady, B et al. 1996; Erber, WN et al. 1997)

⁴¹ (Wigle, DA et al. 1993; Chao, J et al. 1996; van Gijlswijk, RP et al. 1997; Mayer, G et al. 2000; Mayer, G et al. 2001)

⁴² (Hopman, AH et al. 1998)

⁴³ (de Haas, RR et al. 1996)

⁴⁴ (Punnonen, EL et al. 1999)

⁴⁵ (Buki, A et al. 2000)

⁴⁶ (Stanarius, A et al. 1999)

⁴⁷ (Mayer, G et al. 1999; Lee, SW et al. 2005)

⁴⁸ (Mayer, G et al. 1997)

CARD, other above mentioned intrinsic drawbacks of the existing techniques in terms of resolution or reproducibility were not overcome.

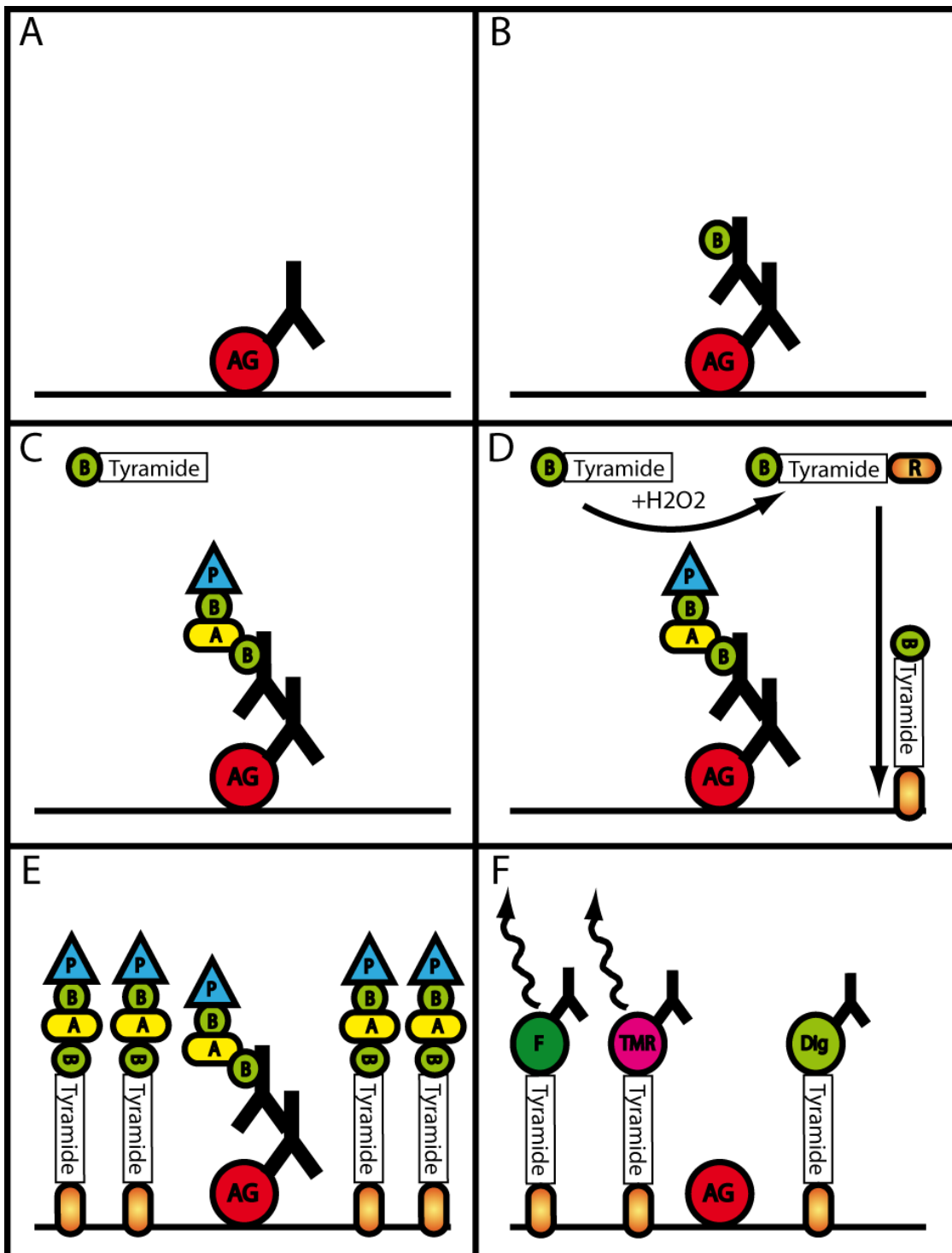


Figure 2: An example of catalyzed reporter deposition (CARD) using a biotin-avidin-peroxidase-system and biotinyl-tyramide. **(A)** An antigen (AG) is labeled with a specific primary antibody. **(B)** A secondary biotin(B) -labeled antibody binds to the primary antibody. **(C)** The avidin-biotinyl-peroxidase (A-B-P) complex binds specifically to the biotin of the secondary antibody. Pre-incubation with biotinyl-tyramide (B-tyramide). **(D)** By adding hydrogen peroxide, biotinyl-tyramide is oxidized leading to the formation of

BT-radicals (*R*), which rapidly and covalently react with proteins surrounding the antigen. **(E)** Thereby, a high amount of biotin is deposited close to the antigen. Deposited biotin is labeled with the avidin-biotinyl-peroxidase (*A-B-P*) complex. Thus, for the following visualization more peroxidase molecules are available resulting in an amplification of the signal. **(F)** Instead of biotin other haptens like digoxigenin (*Dig*), fluoresceine (*F*) and tetramethylrhodamine (*TMR*) can be deposited and labeled with specific antibodies. Fluoresceine and tetramethylrhodamine can also be detected by analysis of their fluorescence signal (*arrows*).

AG= antigen, B=biotin, P=peroxidase, R=radical, F=fluoresceine, TMR=tetramethylrhodamine, Dig=Digoxigenin

Apart from amplification techniques, however, haptens may also be employed for a combination of the pre- and post-embedding technique. In a preliminary study, secondary antibodies labeled with the hapten dinitrophenol were used to localize an antigen in cultured human fibroblast cells (Pathak et al).⁴⁹ After labeling with dinitrophenol-labeled primary and secondary antibodies the cells were osmicated and embedded in epoxy-resin. Following embedding, instead of the original antigen the hapten dinitrophenol was visualized using an anti-dinitrophenol antibody and a colloidal gold-protein-A conjugate. Since with this technique the haptens remain invisible during pre-embedding labeling until visualized by the subsequent post-embedding labeling step, it will be referred to as “virtual pre-embedding” (VirP) in the present thesis (Figure 3). In another, more recent preliminary study⁵⁰, a biotin-CARD step instead of a secondary antibody was used to label an antigen in cell cultures. The deposited and methacrylate embedded biotin was then visualized in a post-embedding step with a colloidal gold conjugated anti-biotin antibody. Thus, the advantages of pre-embedding labeling were combined with the preferred marker for electron microscopy, i.e. sufficiently large colloidal gold particles applied in the final post-embedding step. Moreover, owing to the high sensitivity of the CARD step and excellent contrast of the label, the method seemed especially suited for the visualization of rare antigens.⁵¹

Interestingly enough, besides the high sensitivity, VirP could fulfill also the other above mentioned demands for a novel pre-embedding method: In theory, it would be easy to use and reproducible (HRP-based), would offer good contrast (colloidal gold marker) and would be suited for correlative approaches (fluorescent haptens). However, both previously mentioned studies (Pathak et al; Humbel et al) were applied to cultured cells. Labeling of single cells or cell monolayers is clearly different from labeling on highly complex tissue sections with respect to penetration of antibodies and background labeling. Therefore, for tracing experiments and

⁴⁹ (Pathak, RK et al. 1989)

⁵⁰ (Humbel, BM et al. 1998)

⁵¹ (Humbel, BM et al. 1998)

correlative studies of the CNS, it remained to be shown that a virtual pre-embedding approach would also be compatible with the lipid-rich and rather compact brain tissue.

Based on these considerations, this thesis aimed to investigate first, whether virtual pre-embedding could be successfully applied to rat brain tissue sections after osmication and epoxy-resin embedding. For this purpose several haptens, either coupled to a primary or secondary antibody or deposited by CARD, were studied. Furthermore, the compatibility of virtual pre-embedding with a simultaneous immunogold-silver-enhancement for double-labeling experimental designs was explored. Finally, the potential of virtual pre-embedding with fluorescent haptens for correlative light and electron microscopy was investigated.

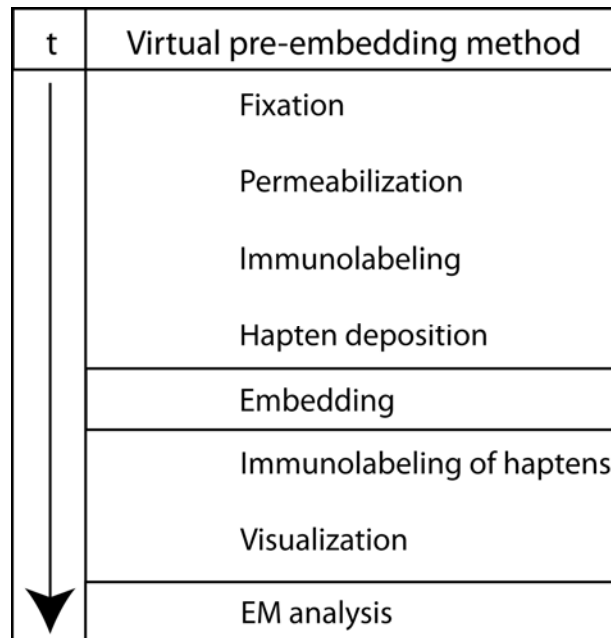


Figure 3: Concept of the virtual pre-embedding labeling technique. Labeling of antigens is accomplished by introduction of haptens into the sections either by haptenylated antibodies or hapten deposition by CARD, respectively. After embedding, the haptens are labeled and visualized by post-embedding techniques.

2 Materials and Methods

2.1 Chemicals and their abbreviations

2,2'-azino-bis(3-ethylbenzthiazoline-6-sulphonic acid (ABTS)	Sigma-Aldrich, Germany
Acetate	Roth, Germany
Acetone	Roth, Germany
Aminosilane	Merck, Germany
Ammonium nickel sulfate (ANS)	Fluka, Germany
Araldite	Serva, Germany
Biotinyl-N-hydroxysuccinimide-ester	Roche, Germany
Bovine hemoglobin	Fluka, Germany
Bovine serum albumin (BSA)	Sigma-Aldrich, Germany
Diaminobenzidine (DAB)	Sigma-Aldrich, Germany
Digoxigenyl-N-hydroxysuccinimide-ester	Roche, Germany
Dimethylformamide (DMF)	Sigma-Aldrich, Germany
Disodium hydrogen phosphate	Merck, Germany
DMP 30	Sigma-Aldrich, Germany
Dodecyl succinic anhydride (DDSA)	Serva, Germany
Entellan	Merck, Germany
Ethanol	Merck, Germany
Fluoresceinyl-N-hydroxysuccinimide-ester	Boehringer-Mannheim, Germany
Glutaraldehyde	Merck, Germany
Gold chloride	Sigma-Aldrich, Germany
Guinea pig immunoglobulin G	Sigma-Aldrich, Germany
Gum arabic	Sigma-Aldrich, Germany
Hydrogen peroxide (HP)	Merck, Germany
Imidazole	Sigma-Aldrich, Germany
Isoflurane	Abbott, Germany
Ketamine	WDT, Germany
Kresyl violet	Sigma-Aldrich, Germany
Lead nitrate	Fluka, Germany
Longasteril	Fresenius, Germany

Methanol	Merck, Germany
Normal goat serum (NGS)	PAN, Germany
Osmium tetroxide	Sigma-Aldrich, Germany
Paraformaldehyde	Electron Microscopic Sciences, USA
Periodic acid	Merck, Germany
Phenylhydrazine	Merck, Germany
Picric acid	Sigma-Aldrich, Germany
Pioloform	Sigma-Aldrich, Germany
Potassium chloride	Merck, Germany
Propylene oxide	Serva, Germany
Q-Sepharose Fast Flow	GE Healthcare
Silver enhancement kit	Amersham, UK
Sodium azide	Merck, Germany
Sodium borohydride	Sigma-Aldrich, Germany
Sodium carbonate	Merck, Germany
Sodium chloride	Merck, Germany
Sodium citrate	Merck, Germany
Sodium dihydrogen phosphate	Merck, Germany
Sodium metaperiodic acid	Merck, Germany
Sodium methoxide	Fluka, Germany
SP-Sepharose Fast Flow	GE Healthcare
Sucrose	Merck, Germany
Texas-Red-N-hydroxysuccinimide-ester	Molecular Probes, USA
Thiomersal	Serva, Germany
Toluene	Merck, Germany
Toluidine blue	Merck, Germany
Triethylamine (TEA)	Sigma-Aldrich, Germany
Tris hydroxymethyl aminomethane (TRIS)	Merck, Germany
Triton X-100	Sigma-Aldrich, Germany
Tyramine-hydrochloride	Sigma-Aldrich, Germany
Uranyl acetate	Merck, Germany
Xylazine	Bayer, Germany
Xylol	J.T. Baker, Netherlands

2.2 Antibodies and their abbreviations

Antibody	Manufacturer	Dot blot	ELISA	Cryo sections	Vibratome sections	Semithin sections	Ultrathin sections
Alexa 568-streptavidin (A568-SA)	MobiTec	X	X	X	X	100	X
Avidin-biotinyl-horseradishperoxidase complex (ELITE ABC)	Vector Laboratories	200	X	200	200	200	200
Biotin-goat anti rabbit (B-GaR)	Vector Laboratories	x	x	2,000	2,000	1,000	x
Biotinyl-rabbit anti mouse (B-HaM)	Vector Laboratories	X	X	2,000	2,000	X	X
Biotinyl-rabbit anti serotonin (B-Ra5HT)	Behringer et al.	100-200	X	100	20	X	X
Digoxigenyl-rabbit anti serotonin (Dig-Ra5HT)	Behringer et al	100-200	X	200	50	X	X
Gold-goat anti mouse 10 nm (Au-GaM 10 nm)	British Biocell International	X	X	X	X	X	50
Gold-goat anti rabbit 1 nm (AuGar 1 nm)	GE Healthcare	X	X	X	100	X	X
Gold-goat anti rabbit 10 nm (Au-GaR 10 nm)	British Biocell International	X	X	X	X	X	50
Horseradishperoxidase streptavidin (P-SA)	Perkin-Elmer	X	10,000	20,000	X	X	X
Horseradishperoxidase streptavidin (P-SA)	SIGMA	X	10,000	X	X	X	X
Horseradishperoxidase-goat anti guinea-pig (P-GaGp)	Jackson	X	10,000	X	X	X	X
Horseradishperoxidase-goat anti rabbit (P-GaR)	Vector Laboratories	x	500	x	x	x	x
Horseradishperoxidase-rabbit anti digoxigenin (P-RaDig)	DAKO	200	X	X	X	X	X
Horseradishperoxidase-rabbit anti fluoresceine (P-RaFlu)	Roche	x	500	X	X	X	X
Horseradishperoxidase-sheep anti digoxigenin (P-ShaDig)	Boehringer	X	500	X	X	X	X
Mouse anti digoxigenin (MaDig)	SIGMA	X	X	10,000	10,000	50	50
Mouse anti fluoresceine (MaFlu)	Boehringer	X	X	X	X	50	50
Mouse anti parvalbumin (MaParv)	SIGMA	x	x	10,000	10,000	x	x
Rabbit anti biotin (RaB)	Veh et al.	X	X	X	X	X	50
Rabbit anti glutamic acid decarboxylase 67 (RaGAD)	Chemicon	X	X	2,000	2,000	X	X
Rabbit anti tetramethylrhodamine (RaTMR)	Molecular Probes	X	500	X	X	200	50
Rabbit anti Texas Red (RaTR)	Molecular Probes	x	500	X	X	X	X

Table 1: Antibodies used in this study. The appropriate dilutions (1:x) are listed when applicable. Antibody against serotonin was the same as that used by Behringer et al.⁵², the purified antibody

⁵² (Behringer, DM et al. 1991)

against biotin was obtained from R.W. Veh. P-SA from Sigma was used only in the experiment described in paragraph 3.2.5.

2.3 Antibody sequences and visualization

	Paragraph	Sequence							
Dot blot assays	3.1.1	B-Ra5HT	ELITE ABC	DAB					
		Dig-Ra5HT	P-RaDig	DAB					
ELISA assays	3.2.1 / 3.2.2	Biotin/P-SA	ABTS						
	3.2.3	P-GaGp	BT	block	P-SA	ABTS			
		P-GaGp	DT	block	P-ShaDig	ABTS			
		P-GaGp	FT	block	P-RaFlu	ABTS			
		P-GaGp	TMRT	block	RaTMR	P-GaR	ABTS		
Cryo sections	3.2.4	MaParv	B-HaM	ABC	BT	block	ABC		
Vibratome sections	3.1.1	B-Ra5HT	embedding						
		Dig-Ra5HT	embedding						
	3.1.2	MaParv	B-HaM	embedding					
	3.2.6	MaParv	B-HaM	ABC	BT	embedding			
	3.2.7	MaParv	B-HaM	ABC	DT	embedding			
		MaParv	B-HaM	ABC	FT	embedding			
	3.2.8	MaParv/RaGAD	AuGaR 1 nm	silver enhancement	B-HaM	ABC	TMRT	embedding	
Semithin sections	3.2.6	ABC	DAB						
	3.2.7	MaDig	B-HaM	DAB					
		MaFlu	B-HaM	DAB					
	3.2.8	RaTMR	B-GaR	DAB					
Ultrathin sections	3.2.6	RaB	AuGaR 10nm						
	3.2.7	MaDig	AuGaM 10nm						
		MaFlu	AuGaM 10nm						
	3.2.8	RaTMR	AuGaR 10nm						

Table 2: Overview over the antibody sequences and the type of visualization used in the different experiments. Description of the experiments is found in the indicated paragraphs. Block= peroxidase block, described in paragraph 2.7.3

2.4 Dot blot assays

Nitrocellulose paper was cut into rectangles with a side length of roughly 2 cm. 1 µl of increasing concentrations (1:200, 1:100 and 1:1) of the haptenylated antibodies (B-Ra5HT, DigRa5HT) were dotted on the nitrocellulose squares. For each assay, the respective cognate antibody served as a control (dilution 1:1). The blots were rinsed in PBS and incubated in 10% NGS for 30 min to saturate unspecific binding sites. After rinsing three times in PBS for 10 minutes, B-Ra5HT labeled nitrocellulose was incubated with ELITE ABC diluted 1:200 in NGS 10% for two hours. Dig-Ra5HT labeled nitrocellulose was incubated in P-RaDig diluted 10% NGS for two hours. After rinsing in PBS three times for 10 minutes, blots were pre-incubated for 15 minutes in DAB solution. Visualization with DAB was achieved by adding ANS (0.3 % final concentration) and hydrogen peroxide (0.0015% final concentration) for 15 minutes in the case of B-Ra5HT labeling and 5 minutes in the case of Dig-Ra5HT labeling, respectively.

PBS*pH 7.4**sodium chloride* *137 mM**potassium chloride* *3 mM**sodiumdihydrogen phosphate* *10 mM***2.5 Synthesis of hapten-tyramides**

Hapten tyramides were synthesized as described by Hopman et al⁵³ with slight modifications. Tyramine-HCL was freshly dissolved prior to the synthesis in DMF to obtain a 50 mM solution. To deprotonate the amino groups of the tyramine 10 µl of TEA was added per 1148 µl of the solution (solution “A”), resulting in a pH between 7 and 8. N-hydroxysuccinimide esters of biotin, digoxigenin, fluoresceine, Texas red and tetramethylrhodamine were freshly dissolved prior synthesis in DMF to obtain a 20 mM solution (solution “B”). 100 µl of solution “A” was thoroughly mixed with 150 µl of solution “B” and 150 µl of DMF and left in the dark for 2 h at room temperature. Subsequently 4.5 ml of ethanol was added to create a 1 mM hapten-tyramide stock solution (Table 3).

Solution A	100 µl	5 µmol of tyramine
Solution B	+ 250 µl	5 µmol of hapten-n-hydroxysuccinimide-ester
DMF	+ 150 µl	reaction solution (10 mM), synthesis for 2 h at room temperature
Ethanol	+ 4500 µl	Hapten-tyramide stock solution (1 mM)

Table 3: Summary of the synthesis of hapten-tyramide conjugates. Activated hapten-esters and tyramine-HCl were incubated at equimolar ratios. By adding ethanol, a 1mM stock solution was prepared.

2.6 Purification of biotinyl-tyramide

⁵³ (Hopman, AH et al. 1998)

A Q-Sepharose column was equilibrated with carbonate buffer 20 mM (pH 9) and loaded with 1.4 ml of BT, diluted 1:2 in carbonate buffer, followed by 5 ml of carbonate buffer and 5 ml of acetate buffer 500 mM (pH 3). A total of 27 fractions were collected (1-7=200 μ l, 8-27=500 μ l per fraction). Fractions containing BT were determined by ELISA (s. paragraph 2.7.1) and pooled.

An SP-Sepharose column was equilibrated with acetate buffer 50 mM (pH 5) and loaded with 1.4 ml of the pool. In total 27 fractions were collected (1-7=200 μ l, 8-27=500 μ l per fraction). Fractions containing BT were determined by ELISA (s. paragraph 2.7.1) and again pooled.

2.7 ELISA assays

2.7.1 Determination of column fractions containing biotinyl-tyramide

Micro titer plates were coated with 100 μ l 1 μ g/ml biotinyl-BSA in coating buffer (*Sodium carbonate 0.05 M, pH 9.6*) overnight at room temperature. Fractions were diluted 1:1,000 in blocking solution (*bovine hemoglobin, 1mg/ml in PBS*) and subsequently diluted 1:10 in HRP-SA 1:10,000, thoroughly mixed and incubated overnight. HRP-SA, diluted 1:10,000, served as a control. The next day, unspecific binding sites on the micro titer plate were blocked with 150 μ l of blocking solution for 1 hour. After washing three times with 200 μ l of PBS, 100 μ l of the HRP-SA treated fractions was applied to the wells for 2 hours. After rinsing three times with PBS, peroxidase activity was visualized using ABTS as a chromogen, diluted 2 mM in incubation buffer (*sodium dihydrogen phosphate 50 mM, sodium acetate 10 mM, pH 4.2*). Hydrogen peroxide was added (0.003 % final concentration) and 100 μ l of solution applied to each well. After 5 minutes the reaction was stopped using 100 μ l of 0.1 % sodium azide. Optical density was measured using a photometer (reader HT2, athmos labtec instruments, Austria). Optical density of the control served as a defined maximum. Optical densities of the fractions were subtracted from the maximum and 3 fractions with highest remaining optical density, containing BT, were pooled.

2.7.2 Determination of the concentration of purified biotinyl-tyramide

To determine the concentration of purified biotinyl-tyramide, an ELISA assay was performed as described in paragraph 2.7.1. Known concentrations of biotin used to block HRP-SA served to create a calibration curve. Based on the equation $\text{ratio} = c/\text{OD}$, OD being the optical density, the ratio for each concentration of biotin was determined and the mean value of the ratios was calculated. Pooled purified BT was used to block HRP-SA in different concentrations estimated to fit in the range of the comparison curve on the basis of the theoretical concentration after the passage of the column (300 μM). Then the mean ratio was used to determine the concentration value for each pool dilution depending on the measured optical density by arranging the above equation as follows: $c = \text{OD} * \text{ratio}$. The mean value of the determined concentrations was calculated yielding the final concentration for the pool.

2.7.3 ELISA model system for the visualization of hapten-tyramides

Micro titer plates were coated with 100 μl 1 $\mu\text{g}/\text{ml}$ guinea pig immunoglobulin G in coating buffer (s. paragraph 2.7.1) overnight at room temperature. The next day unspecific binding sites were blocked with 150 μl of blocking solution (s. paragraph 2.7.1) for 1 hour. After washing three times with 200 μl of PBS, 100 μl of a peroxidase-labeled goat anti guinea pig antibody, diluted 1:10,000 in blocking solution, was applied to the wells for 2 hours. After washing three times with 200 μl of PBS, 100 μl of hapten-tyramides, diluted at different molarities in CARD-solution (s. paragraph 2.8.2) was applied to the wells. Deposition of hapten-tyramides was accomplished by adding hydrogen peroxide (0.0015% final concentration) and incubation for 15 minutes. Subsequently, peroxidase activity was completely blocked by the use of 200 μl of 1% sodium azide and 1% hydrogen peroxide in PBS for 10 min, followed by 0.05% phenylhydrazine in PBS for 30 minutes.⁵⁴ After thorough rinsing, deposited haptens were labeled with 100 μl of hapten-specific antibodies or HRP-SA, adequately diluted in blocking solution for 2 hours. Antibodies were either already labeled with peroxidase or were labeled with a peroxidase-linked secondary antibody in an additional step. After rinsing three times with PBS, peroxidase activity was visualized using ABTS as a chromogen, diluted to 2 mM in incubation buffer (s. paragraph 2.7.1). Hydrogen peroxide was added (0.003 % final concentration) and 100 μl of the solution

⁵⁴ (Li, CY et al. 1987)

applied to each well. After 5 minutes the reaction was stopped using 100 μ l of 0.1 % sodium azide. Optical density was measured using a photometer (reader HT2, athmos labtec instruments, Austria).

2.8 Immunocytochemistry

2.8.1 Perfusion fixation

Adult Wistar rats were pre-anesthetized in a chamber with 2% isoflurane and then deeply anesthetized by an intraperitoneal injection of ketamine and xylazine. Heparin was added as a coagulation inhibitor. All drug doses were adjusted according to body weight (45% ketamine, 35% xylazine and 20% saline; 0.16ml/100 g body weight). The animals were consequently perfused transcardially with

- Longasteril[®] (plasma expander) for 10 seconds at 28 kPa (210 torr)
- fixation solution (PGPic) for 5 minutes at 28 kPa
- fixation solution (PGPic) for 25 minutes at 28 kPa
- phosphate buffered sucrose solution for 5 minutes at 2.7 kPa

After perfusion, brains were removed from the skull. For light microscopy, they were subsequently embedded in a 2% agarose solution for support and cut transversely into 2-10 mm thick blocks, which were then cryo-protected in 0.4 M sucrose solution (*sucrose 146 mM, sodium dihydrogen phosphate 100 mM, pH 7.4*) for 1 hour, followed by a 0,8 M sucrose solution overnight. The blocks were mounted on cork plates, frozen in hexane at -60 °C, and stored at -80 °C until use.

For electron microscopy, brains were immediately sectioned on a vibratome.

PGPic

pH 7.4

<i>paraformaldehyde</i>	<i>4% (w/v)</i>	<i>sodium dihydrogen</i>	
<i>glutaraldehyde</i>	<i>0.05% (w/v)</i>	<i>phosphate</i>	<i>100 mM</i>
<i>picric acid</i>	<i>0.37%</i>		

2.8.2 Cryostat sections for light microscopy

Frozen brain tissue was sectioned at 20 μm thickness using a cryostat microtome, washed several times in PBS, and then treated with 1% sodium borohydride in PBS for 15 minutes to inactivate remaining aldehyde groups. After two washing steps in PBS for 15 minutes each, sections were pre-incubated for 30 minutes in 10% normal goat serum in PBS to saturate unspecific binding sites, containing 0.3 % triton for permeabilization and 0.05% phenylhydrazine to block endogenous peroxidase activity. Subsequently, the sections were incubated for at least 36 hours at 4 °C in the primary antibody solution, containing 10% NGS in PBS, 0.3% triton, 0.1% sodium azide and 0.01% thiomersal for preservation and the appropriately diluted primary antibody. Sections were rinsed twice for 20 and 40 minutes in PBS, followed by pre-incubation with PBS-A for 1 hour and incubation overnight at 4 °C with the biotinylated secondary antibody diluted in PBS-A. After two washing steps in PBS for 20 and 40 minutes and pre-incubation in PBS-A for 1 hour, sections were incubated overnight at 4 °C with ELITE ABC. After rinsing in PBS three times for 10, 20 and 30 minutes, sections were pre-incubated for 15 minutes in DAB or tyramide-conjugates, appropriately diluted in CARD-solution. Visualization with DAB was achieved by adding ANS (0.3 % final concentration) and hydrogen peroxide (0,0015% final concentration) for 15 minutes. Deposition of hapten-tyramide was achieved by adding only hydrogen peroxide for 15 minutes.

For the visualization of deposited biotinyl-tyramide, first the ELITE ABC peroxidase activity was then blocked by a mixture of 1% sodium azide and 1% hydrogen peroxide in PBS for 10 minutes, followed by 0.05% phenylhydrazine in PBS for 30 minutes. After rinsing for several times in PBS, sections were preincubated in PBS-A for 1 hour and incubated again overnight at 4 °C in a dilution of ELITE ABC in PBS-A. Deposited biotin was visualized with DAB as described above.

After rinsing several times, slices were mounted onto gelatin-coated slides and air-dried for 30 minutes, followed by a dehydration in an ascending series of ethanol. They were then transferred to xylene and cover-slipped with entellan.

PBS-A

Bovine serum albumin 2% (w/v) in PBS

TRIS-Buffer

pH 7.6

TRIS.

50mM

<i>CARD-solution</i>	<i>in H₂O</i>	<i>DAB-solution</i>	<i>in H₂O</i>
<i>TRIS-buffer</i>	<i>50 mM</i>	<i>TRIS-buffer</i>	<i>50 mM</i>
<i>Imidazole</i>	<i>10 mM</i>	<i>Imidazole</i>	<i>10 mM</i>
		<i>DAB</i>	<i>1.2 mM</i>

2.8.3 Analysis of cryostat sections for light microscopy

Images were recorded using a Leica microscope (DMRB, Leica, Germany), a CCD-camera (CX9000, MBF Bioscience, USA) and Neurolucida software (Version 8.10, MBF Bioscience, USA).

Images of the fluorescence signal were recorded using a Leica microscope (DMLB, Leica, Germany), a CCD-camera (DFL490, Leica, Germany) and Leica application suite software (Version 2.8.1, Leica, Germany).

2.8.4 Vibratome sections for virtual pre-embedding

Freshly perfused brain tissue was sectioned at 50 μ m thickness using a vibratome. Sections were rinsed several times in PBS, followed by incubation in 20% sucrose in 0.1 M phosphate buffer twice for 10 min. They were then transferred on a plastic support and freeze-thawed using liquid nitrogen.⁵⁵ Pre-treatment of the sections and incubation with the primary antibody were performed as previously described (paragraph 2.8.2) with the following exceptions: 0.1% sodium borohydride and 0.05% triton were used for pre-incubation and incubation, respectively. Rinsing, incubation with the secondary antibody and deposition of hapten-tyramides was carried out as described above (paragraph 2.8.2).

In virtual pre-embedding with haptenylated primary antibodies only (see paragraph 3.1), incubation with the primary antibody lasted for at least 36 hours. In virtual pre-embedding with haptenylated secondary antibodies (s. paragraph 3.2), secondary antibodies were incubated overnight. The tissue with haptens deposited either with haptenylated primary antibodies, haptenylated secondary antibodies or CARD was then embedded in araldite according to standard procedures (s. paragraph 2.8.7).

⁵⁵ (Lujan, R et al. 1997)

Phosphate buffer 0.1 M*pH 7.4**sodium dihydrogen phosphate 100 mM**disodium hydrogen phosphate 100 mM***2.8.5 Double labeled brain sections for virtual pre-embedding and correlative microscopy**

For double labeling, 50 µm thick vibratome sections were pre-treated as previously described (paragraph 2.8.4). Sections were then simultaneously incubated with the primary antibodies, e.g. MaParv and RaGAD, for at least 36 hours at 4 °C in a solution containing 10% normal goat serum in PBS, 0,05% triton, 0,1% sodium azide and 0.01% thiomersal. Subsequently sections were rinsed twice for 20 and 40 minutes in PBS, followed by pre-incubation with PBS-A for 1 hour and incubation overnight at 4 °C with 1 nm AuGaR. After rinsing in PBS three times for 10, 20 and 30 minutes, sections were rinsed 5 times in 150 mM sodium nitrate to remove chloride molecules. A commercial silver enhancement kit (Amersham) was used according to the instructions of the manufacturer, except that one third of gum arabic was added. Sections were incubated in the silver enhancement solution for 20-30 minutes under visual control. After rinsing three times in 150 mM sodium nitrate for 10 minutes, sections were treated with 150 mM acetate buffer (pH 5), followed by a gold toning with 0.05 % gold chloride in 150 mM acetate buffer at 0°C. After thorough rinsing with acetate buffer and PBS, sections were pre-incubated with PBS-A for 1 hour and incubated overnight at 4 °C with B-HaM in PBS-A. Deposition of tetramethylrhodamine-tyramide (10 µM) was achieved as described in paragraph 2.8.2.

2.8.6 Analysis of double labeling and correlation studies

Light microscopic bright field and fluorescence images were recorded either using a Leica microscope (DMRB, Leica, Germany), a CCD-camera (CX9000, MBF Bioscience, USA) and Neurolucida software (Version 8.10, MBF Bioscience, USA) or a Leica microscope (DMLB, Leica, Germany), a CCD-camera (DFL490, Leica, Germany) and Leica application suite software (Version 2.8.1., Leica, Germany). The second equipment set was used for the analysis of fluorescent CARD signals.

2.8.7 Embedding in araldite

Sections were post-fixed with 1% osmium tetroxide in 0.1 M phosphate buffer for 10 minutes and washed in phosphate buffer. They were then dehydrated in graded series of ethanol for 5 minutes per step (1x50%, 2x70%), block stained in 2% uranyl acetate in 70% ethanol for 30 minutes, followed by further dehydration for 5 minutes per step (2x70%, 2x80%, 2x90%, 2x95%, 3x100%). Sections were transferred into 100% propylene oxide twice for 10 minutes, followed by incubation in a 1:1 mixture of propylene oxide and araldite (*Pure araldite and dodecenyl succinic anhydride mixed in a ratio of 30:24*) with 1.5 % DMP 30 overnight under constant agitation. The next day, the embedding solution was prepared (*2% DMP 30 in araldite, gently stirred for 30 minutes with a glass rod*). Sections were transferred to fresh embedding solution twice for 2 hours before flat-embedding them sandwiched between a sheet of aclar plastic and an araldite slide. Slices were then polymerized overnight at 60° C.

2.8.8 Preparation of semithin and ultrathin sections

Regions of interest were cut out from the polymerized sections and mounted for sectioning. Semithin (500 nm) and ultrathin sections (60-70 nm) were cut alternately using a diamond knife (Diatome, Switzerland) and an ultramicrotome (Reichert Ultracut S, Leica, Germany). Semithin sections were dried at 70 °C to aminosilane-coated slides. Ultrathin sections were collected on 0.75% pioloform-coated 200 to 300 mesh nickel grids.

2.8.9 Post-embedding immunocytochemistry on semithin sections

For post-embedding labeling, sections were incubated in methanolate etching solution (*sodium methoxide 1 M in a 2:1 mixture of methanol and toluene*) for 10 minutes, followed by rinsing in a 1:1 mixture of methanol and toluene for 5 minutes and twice in acetone for 5 minutes. After rinsing with distilled water, slides were transferred for a few minutes in 100 mM acetate buffer (pH 5). Afterwards, sections were incubated in 2% hydrogen peroxide for 5 minutes, transferred again into acetate buffer for several minutes and finally rinsed in PBS.

Slides were then transferred into a humid chamber. All subsequent steps were performed at room temperature. Sections were pre-incubated in 10% NGS for 30 minutes, followed by incubation with the appropriately diluted primary antibody (in 10% NGS) overnight. After rinsing twice for

5 and 10 minutes in PBS, sections were pre-incubated in PBS-A for 15 minutes and then with the appropriately diluted secondary antibody (in PBS-A) for 4 hours. Having been rinsed again twice for 5 and 10 minutes in PBS and pre-incubation in PBS-A, sections were incubated with ELITE ABC in PBS-A for 1 hour. After washing twice in PBS for 5 and 10 minutes, sections were pre-incubated in DAB-solution for 15 minutes. Visualization was performed as described in paragraph 2.8.2. In double-labeling experiments involving silver-enhanced particles, ANS was not used.

For the visualization of CARD-deposited biotin, Elite ABC was used, followed by visualization with DAB. Alternatively, a fluorophore-linked streptavidin was used to visualize biotin.

In control experiments the primary antibody or Elite ABC were omitted.

2.8.10 Staining of semithin sections

Sections parallel to immunocytochemically treated sections were stained with toluidine blue (*toluidine blue 1% w/v, sodium borohydride 1% w/v, Sucrose 40% w/v*). The sections were incubated in toluidine blue solution for 3 minutes at 70° C, then thoroughly washed in distilled water, dried at 70 °C and cover-slipped in entellan.

2.8.11 Post-embedding immunocytochemistry on ultrathin sections

All steps were performed at room temperature. Grids with the sections facing downward were placed on 50 µl-droplets of distilled water on a sheet of parafilm. The grids were then transferred from droplet to droplet. Unmasking of epitopes to reverse the effect of osmium tetroxide was performed by incubation in 1% periodic acid, washing in H₂O, followed by incubation in 1% sodium metaperiodic acid. Subsequently, the grids were jet-rinsed with distilled water and transferred to a silicone embedding form with cavities able to hold about 25 µl of solution. Solutions were changed by moving the grids to adjacent cavities. Grids with the sections facing upward, were incubated in TBSX (*TRIS 50 mM, Triton x-100, sodium hydrochloride 139 mM*) for 10 minutes, followed by pre-incubation in Block 1 for 30 minutes. The primary antibody was appropriately diluted in Block 1 (*normal goat serum 5%, bovine serum albumin 2%, in TBSX*) and the grids were incubated overnight. The next day, sections were jet rinsed with TBSX twice, pre-incubated in Block 2 (*bovine serum albumin 2%, in TBSX*) for 10 minutes and incubated in the

secondary antibody solution (secondary gold colloid-conjugated antibody, appropriately diluted in Block 2) for 90 minutes. Grids were then jet-rinsed twice in TBSX, once in distilled water, and air-dried.

2.8.12 Staining of ultrathin sections

Grids, sections facing downward, were placed on droplets of 2% uranyl acetate in 70% ethanol for 5 minutes. Afterwards, grids were jet-rinsed with H₂O and air-dried. Double staining was performed using lead citrate as described by Reynolds⁵⁶ (*H₂O 5 ml, lead nitrate 133 mg, sodium citrate 200 mg, sodium hydroxide 10 N 75 μl*) for 20 seconds, again followed by jet-rinsing with H₂O and air drying.

2.8.13 Analysis of ultrathin sections

Sections were examined using a Leo 912 transmission electron microscope (Leica Electron Optics, Germany). Images were recorded using a CCD-camera (Proscan 1K, Proscan, Germany) and iTEM Software (Version 5.0, Olympus Soft Imaging Solutions, Germany).

⁵⁶ (Reynolds, ES 1963)

3. Results

3.1 Virtual pre-embedding with haptenylated antibodies

Haptens can be introduced into brain tissue sections either by means of haptenylated primary or secondary antibodies or by CARD amplification. In comparison to the highly sensitive CARD system, it can be expected that the use of a haptenylated secondary or primary antibody should clearly be less sensitive. It may, however, still be an appropriate method to label and visualize abundant antigens or tracers. Therefore, the use of haptenylated antibodies for VirP in rat brain tissue sections was investigated.

3.1.1 Biotinylated and digoxigenylated primary antibodies are not suited for virtual pre-embedding in rat brain sections

Previously characterized⁵⁷ biotinylated and digoxigenylated primary rabbit antibodies against serotonin (B-Ra5-HT, Dig-Ra5-HT) were used as haptenylated primary antibodies. Successful haptenylation of the antibodies was verified by a dot blot assay. As expected, staining intensity increased with increasing concentrations of the antibodies (Figure 4, A).

With LM immunocytochemistry, both haptenylated antibodies were used at previously determined optimal dilutions (B-Ra5HT: 1:100 , Dig-Ra5-HT: 1:200, data not shown). Anti-species and anti-hapten immunoreactivity served as positive controls and specifically stained serotonergic neurons of the dorsal raphe (Figure 4, B-F). Staining intensity in 50 μm vibratome sections (Figure 4, D and F) was comparable with 25 μm cryosections (Figure 4, C and E) . With regard to superior ultrastructural preservation, vibratome sections were chosen for subsequent virtual pre-embedding labeling.

To avoid false negative labeling, higher concentrations of the antibodies were chosen for virtual pre-embedding labeling (B-Ra5HT: 1:20, Dig-Ra5HT: 1:50) compared with LM immunocytochemistry. After embedding in araldite, however, neither biotin nor digoxigenin were detected via post-embedding labeling on semithin and ultrathin sections (data not shown).

⁵⁷ (Behringer, DM et al. 1991)

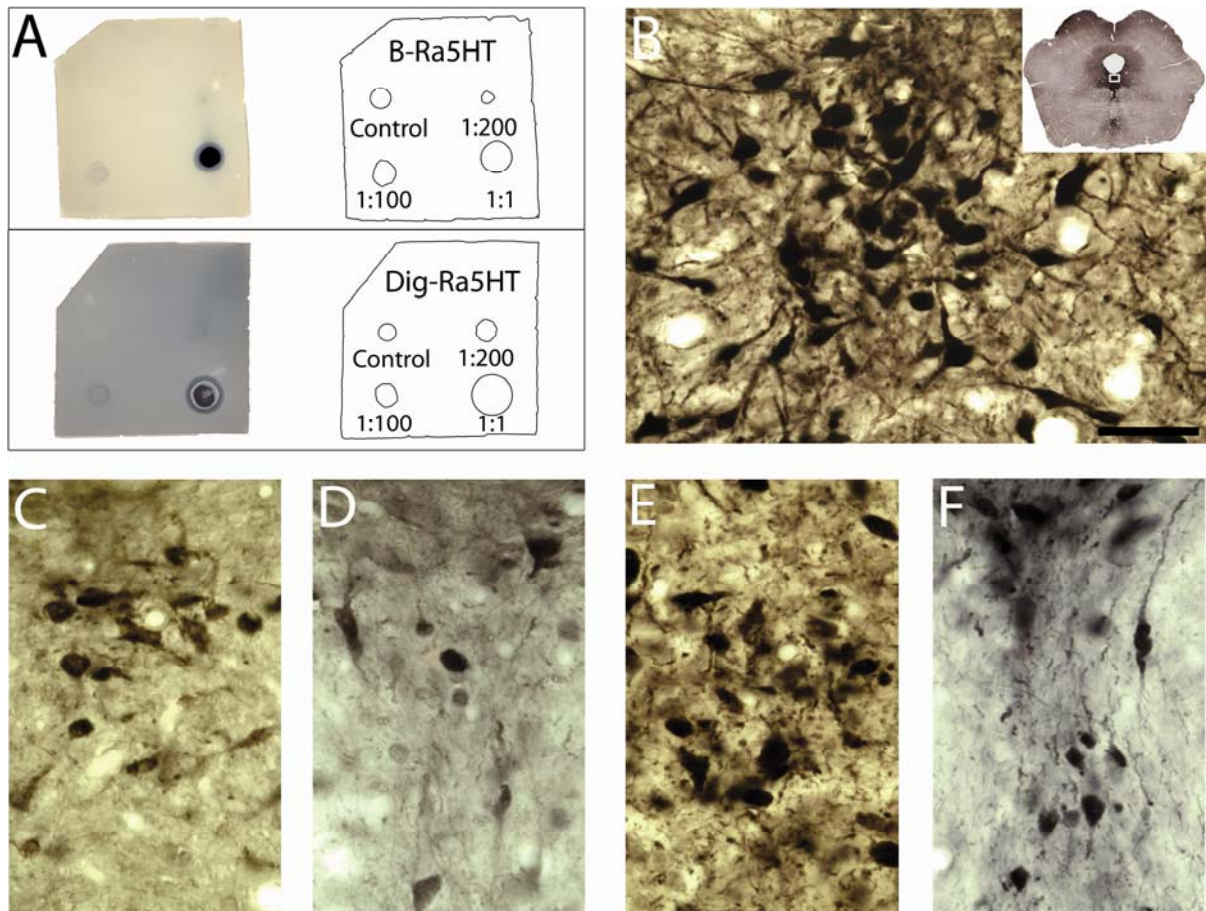


Figure 4: Virtual pre-embedding with biotinylated and digoxigenylated primary antibodies against 5HT (B-Ra5HT or Dig-Ra5HT). **(A)** A dot blot assay confirmed haptenylation of both antibodies by clear visualization of both haptens in a concentration dependent manner (negative control, 1:200, 1:100, 1:1) by specific anti-biotin and anti-digoxigenin immunoreactivity. **(B)** Visualization of the rabbit antibodies served as positive control displaying serotonergic neurons of the dorsal raphe nuclei in cryosections (25 μm) of the rat brainstem. Position of the displayed area is indicated by the white box in the inset. **(C)** By comparison, visualization of the biotin moieties of the biotinylated primary antibody in cryosections (25 μm) displayed 5HT containing cell bodies clearly but less intensely. Labeled neuronal processes were largely not detected. **(D)** In vibratome sections (50 μm) staining intensity was comparable to C, but clearly less neurons were detected. **(E)** Visualization of digoxigenin moieties of the digoxigenylated primary antibody in cryosections (25 μm) resulted in a similar pattern of immunoreactivity as in C, though more processes were observed than with anti-biotin labeling. **(F)** In accordance with D, on vibratome sections (50 μm) staining intensity was not diminished, but less neurons with labeling were visible. However, with virtual pre-embedding after embedding in araldite neither hapten was detected by post-embedding labeling (data not shown). Scale bar indicates 30 μm (B-F).

3.1.2 A biotinylated secondary antibody provides a weak, but specific signal with virtual pre-embedding

Assuming that the detection of haptens coupled to primary antibodies was limited by low availability of hapten epitopes, a more sensitive indirect labeling approach with a haptenylated secondary antibody was tested next. For this purpose, the calcium binding protein parvalbumin was indirectly labeled with a biotinylated secondary antibody. Light microscopic visualization with the ABC/DAB procedure served as positive control. The characteristic pattern of parvalbumin immunoreactivity consisting of intensely labeled cells and a delicate network of neuronal processes was evident in rat cerebral neocortex (Figure 5, A-C).

With virtual pre-embedding detecting embedded biotin, a similar pattern of stained cells and processes was observed in semithin sections (Figure 5, D-F).

Correspondingly, in adjacent ultrathin sections, biotin was specifically, but relatively weakly visualized in the cytoplasm and nucleus of cell bodies and in axonal terminals via immunogold labeling (Figure 5, G-H).

3.2 Virtual pre-embedding with CARD

Using the CARD technique to introduce haptens into the tissue, an increase in sensitivity and therefore in the signal-strength may be expected in comparison with haptenylated secondary antibodies. However, to achieve optimal deposition of haptens, the specific biochemical characteristics of the distinct hapten-tyramides (biotin-, digoxigenin-, fluorescein- and tetramethylrhodamine-tyramide) as peroxidase-substrates had to be explored before their use in virtual pre-embedding labeling.

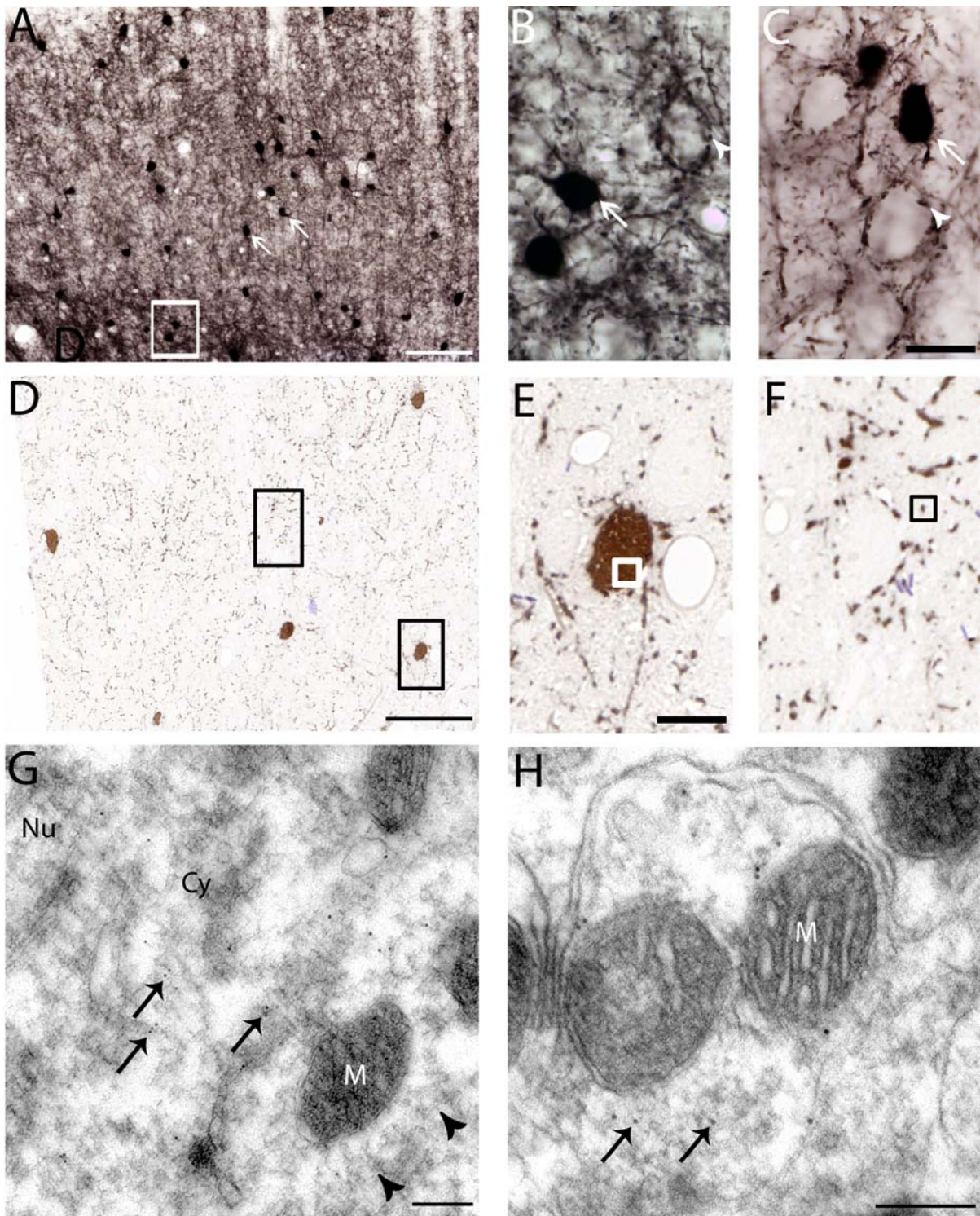


Figure 5: Virtual pre-embedding with a biotinylated secondary antibody. Parvalbumin, a calcium binding protein, was labeled. (A) Light microscopic positive control with visualization by DAB displaying parvalbumin immunoreactivity in a 25 μm cryosection of the rat cerebral cortex. Parvalbumin positive somata (arrows) and numerous neuronal processes were detected. The boxed area is shown at higher magnification in B. (B) High magnification with parvalbumin immunopositive somata (arrow). Punctate profiles likely to represent axosomatic terminals were also observed (arrowhead). (C) In vibratome sections (50 μm) labeling intensity was somewhat lower when compared to B, but neurons (arrow) and axosomatic terminals (arrowhead) were still strongly labeled. (D) With virtual pre-embedding, post-embedding visualization of biotin by DAB on semithin (500

nm) sections of the neocortex resulted in a very similar parvalbumin-specific pattern of immunoreactivity. Boxed areas in D are shown at higher magnification in E and F. At higher magnification (E, F), aside from parvalbumin positive somata, elongated and punctate immunoreactivity profiles were readily depicted. The boxed area in E is shown at higher magnification in G. (G) Post-embedding visualization of biotin using 10 nm colloidal gold in adjacent ultrathin sections (70 nm). The area shown is marked by the boxed area in E. The cytoplasm (Cy) of the identified parvalbumin-positive interneuron shows a specific, but relatively weak labeling (arrows). The cell border is indicated by arrowheads. (H) The terminal located in the boxed area in E similarly displayed a specific, but rather weak labeling (arrows). Scale bars indicate 100 μm (A), 10 μm (B), 60 μm (C), 10 μm (D,E), 500 nm (F), 200 nm (G). Cy=cytoplasm, M=Mitochondrion, Nu=Nucleus

3.2.1 Purified hapten-tyramide conjugates have no benefit in comparison with unpurified conjugates

Although equimolar ratios of haptens and tyramide were used for synthesis (see paragraph 2.5 of the methods section), residual free activated hapten or free tyramide could possibly interfere with the CARD reaction. Therefore, excess free biotin was removed on a Q-sepharose-column and excess free tyramine was removed on a SP-sepharose-column. The concentration of purified biotinyl-tyramide was determined by ELISA (data not shown).

To test for a possible benefit resulting from purification, the concentration dependent deposition of purified vs. unpurified biotinyl-tyramide conjugate was compared in a CARD-ELISA assay. Similarly shaped concentration dependent enzyme activity curves were measured for both substrates. A plateau of maximum activity between 6-10 μM was followed by a decrease in activity above 12 μM . However, enzyme activity with the unpurified substrate rose more steeply and sustained higher activity at concentrations above 2 μM (Figure 6, A). Based on these results, the non-purified hapten-conjugates were chosen for all subsequent experiments.

3.2.2 Synthesized biotinyl-tyramide is superior to purchased biotinyl-tyramide

In an ELISA assay, the CARD signal intensity achieved with synthesized biotinyl-tyramide was compared with the signal intensity obtained with a commercially available CARD amplification system (NEN-kit). Biotin deposited with either substrate was visualized using two different horseradish labeled streptavidin conjugates (HRP-SA), one purchased from Sigma and the other included in the NEN-kit. Enzyme activity obtained with the commercial kit was by 10% (NEN-

HRP-SA) and 21% (Sigma-HRP-SA), respectively, lower than the activity obtained with synthesized BT (Figure 6, B).

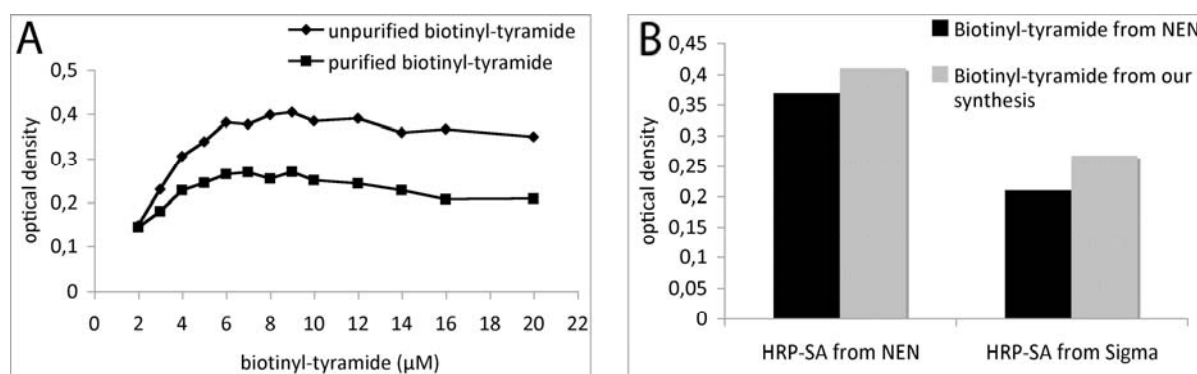


Figure 6: (A) Comparison of enzyme activity achieved with use of purified versus unpurified BT as a peroxidase substrate visualized by ABTS in an ELISA assay. Though both conjugates showed a substrate concentration dependent activity with a steep rise in activity until 6 μM followed by a decline at concentrations above 10 μM , unpurified BT yielded an increased optical density when compared to purified BT. Optimal substrate concentrations were observed between 6-10 μM . (B) Comparison of enzyme activity achieved with unpurified BT (striped columns) versus BT from a commercially available amplification kit (black columns). Deposited BT was visualized using either horseradish peroxidase-labeled streptavidin (HRP-SA) from the kit or a commercially available HRP-SA. With both HRP-SA reagents, BT from the commercial kit was less effective by 10% and 21%, respectively, than BT from our synthesis. Unpurified BT was used at 5 μM , BT (NEN kit) was used according to the instructions of the manufacturer.

3.2.3 CARD signal intensity in ELISA-assays is dependent on the hapten-tyramide concentration

In CARD-ELISA assays, similarly shaped concentration dependent enzyme activity curves were observed using Texas-Red-tyramide (TT) and tetramethylrhodamine-tyramide (TMRT) conjugates. A steep increase was followed by an optimal concentration range between 2 and 10 μM with a subsequent drop at higher concentrations (Figure 7, B and D).

The shape of curves and concentration range optima were substantially different for fluoresceine-tyramide (FT) and digoxigenyl-tyramide (DT). Whereas the activity curve with FT peaked around 4 μM with a subsequent increase in activity at very high concentrations, with DT a sharp peak around 3 μM and a more restricted optimal range than observed with the other conjugates was found (Figure 7, A and C).

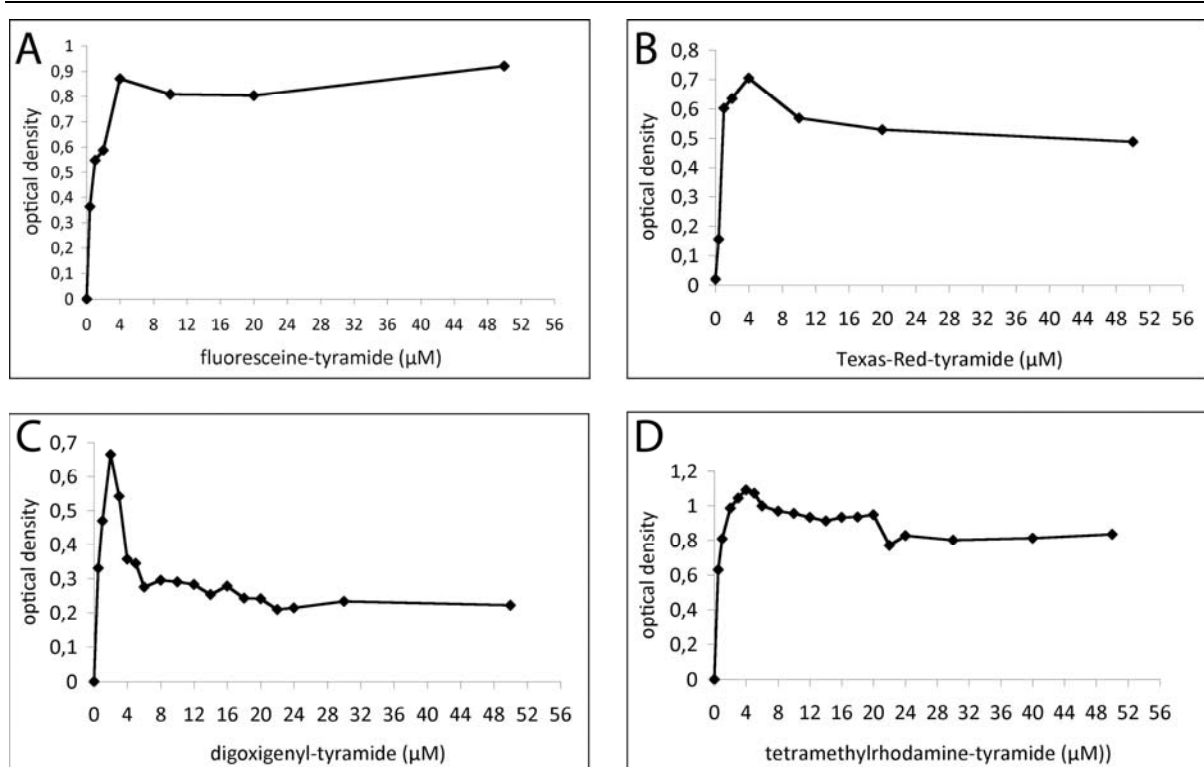


Figure 7: Enzyme activity achieved with use of different haptent-tyramides as peroxidase substrates visualized by ABTS in an ELISA assay (A) Fluorescein-tyramide as a substrate was characterized by a steep increase in peroxidase activity up to 4 μM , followed by a plateau at a slightly decreased level and again a moderate increase at very high substrate concentrations. (B) Texas-Red-tyramide (TT) showed a peak of peroxidase activity at 5 μM , the optimal range lying between 1-12 μM . (C) Digoxigenin-tyramide resulted in a sharp peak at 3 μM . When compared to TT, the optimal concentration range was more narrowly defined to 0.5 to 5 μM . (D) By comparison, tetramethylrhodamine-tyramide showed similar characteristics as TT (peak at 4 μM ; range between 2-10 μM).

3.2.4 CARD signal intensity in immunocytochemistry is also dependent on the haptent-tyramide concentration

To test whether the substrate-concentration dependence of haptent-tyramides as observed with ELISA assays (s. 3.2.3) also applied for immunocytochemistry, parvalbumin was visualized in rat pallidum by BT-CARD. Biotin was deposited using different concentrations of BT (1, 5 and 20 μM) and visualized by the ABC/DAB procedure. With a BT concentration of 1 μM , staining of neuronal cell bodies was strong and neuronal processes were readily distinguishable, whereas no background signal was evident. (Figure 8, B). With a concentration of 5 μM , not only neuronal cell bodies, but also neuronal processes were intensely labeled. Background staining was also low (Figure 8, C). When using 20 μM of BT, labeling intensity of neuronal cell bodies and processes was less pronounced than with 1 and 5 μM , while background staining became evident (Figure 8, D).

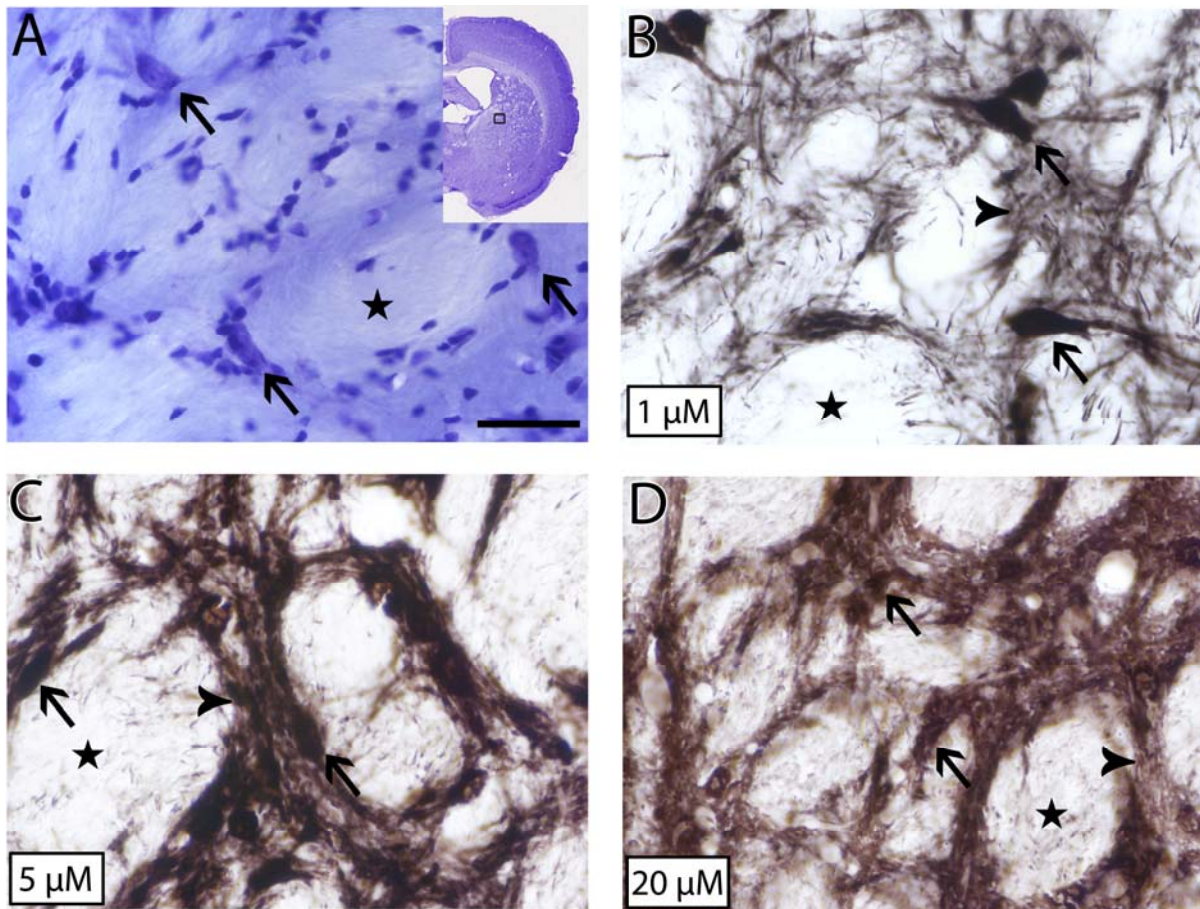


Figure 8: Characterization of biotinyl-tyramide (BT) as a peroxidase substrate in light microscopy visualized by the ABC/DAB procedure in rat pallidum. Parvalbumin immunolabeling. **(A)** In a cresyl-violet stained section, next to fiber tracts (asterisk) oval-shaped comparatively large neurons (arrows) could be observed. Inset: boxed area indicates the area shown in A. **(B)** With BT at 1 μM parvalbuminergic neurons (arrows) were clearly visualized among labeled processes (arrowhead). No background labeling was evident in the fiber tracts (asterisk). **(C)** With an increased BT substrate concentration of 5 μM neuronal cell bodies (arrow) were strongly stained and the neuropil labeling was considerably increased (arrowhead). Under these conditions, background labeling was still relatively low (asterisk). **(D)** BT at 20 μM resulted in a decreased labeling intensity and a granulated staining pattern in neurons (arrows) and neuropil (arrowhead). In fiber tracts, an increased background staining was evident (asterisk). Scale bar indicates 30 μm .

3.2.5 Peroxidase-conjugated streptavidin is not suited for virtual pre-embedding

In preliminary virtual pre-embedding experiments with BT deposited by horseradish-peroxidase labeled streptavidin (HRP-SA), the signal seemed to be largely restricted to the surface of the sections (data not shown). Therefore, penetration characteristics of HRP-SA in comparison with the avidin-biotinylperoxidase complex (ELITE ABC) were investigated. For this purpose, biotin deposited either by HRP-SA or ELITE ABC was visualized in semithin cross-sections of 30 μm

thick cryostat slices. With HRP-SA, the penetration depth was limited to only a few microns (Figure 9, A). With ELITE ABC, by contrast, biotin could be detected throughout the whole depth of the section (Figure 9, B). Based on these results ELITE ABC was chosen for all subsequent virtual pre-embedding experiments.

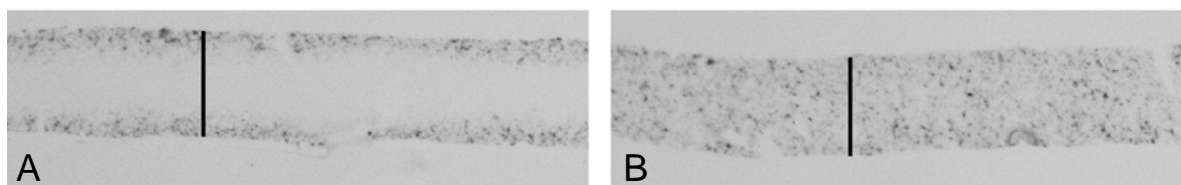


Figure 9: Penetration properties of horseradish-labeled streptavidin (HRP-SA) and avidin-biotinyl-peroxidase complex (Elite ABC) in virtual pre-embedding with BT in cross sectioned cryostat sections (30 μm). Glutamic acid decarboxylase (GAD67) post-embedding immunoreactivity was visualized by DAB. Penetration depth of HRP-SA (**A**) was limited to a few microns, whereas with Elite ABC (**B**) biotin was detected throughout the whole depth of the section. Vertical bars indicate 22 μm in A and 21 μm in B.

3.2.6 Biotinyl-tyramide CARD provides a strong and highly specific signal with virtual pre-embedding in rat brain sections

After determination of optimal biochemical characteristics of hapten-tyramides, the feasibility of virtual pre-embedding with CARD was investigated with BT at a concentration of 5 μM (compare 3.2.4). In analogy to the previous experiments, parvalbumin was detected. After embedding in araldite, visualization of biotin by either the ABC/DAB procedure or fluorescence microscopy displayed the characteristic parvalbumin staining pattern in semithin sections of rat neocortex (Figure 10, A-C; Figure 11, A and B; compare Figure 5, A-C). Comparison with adjacent toluidine-blue stained sections allowed for correlation of labeled profiles and neuronal structures (Figure 10, D).

In 70 nm thick ultrathin sections, colloidal gold labeling of cell bodies and axo-somatic terminals was dense and highly distinct (Figure 11, C and D).

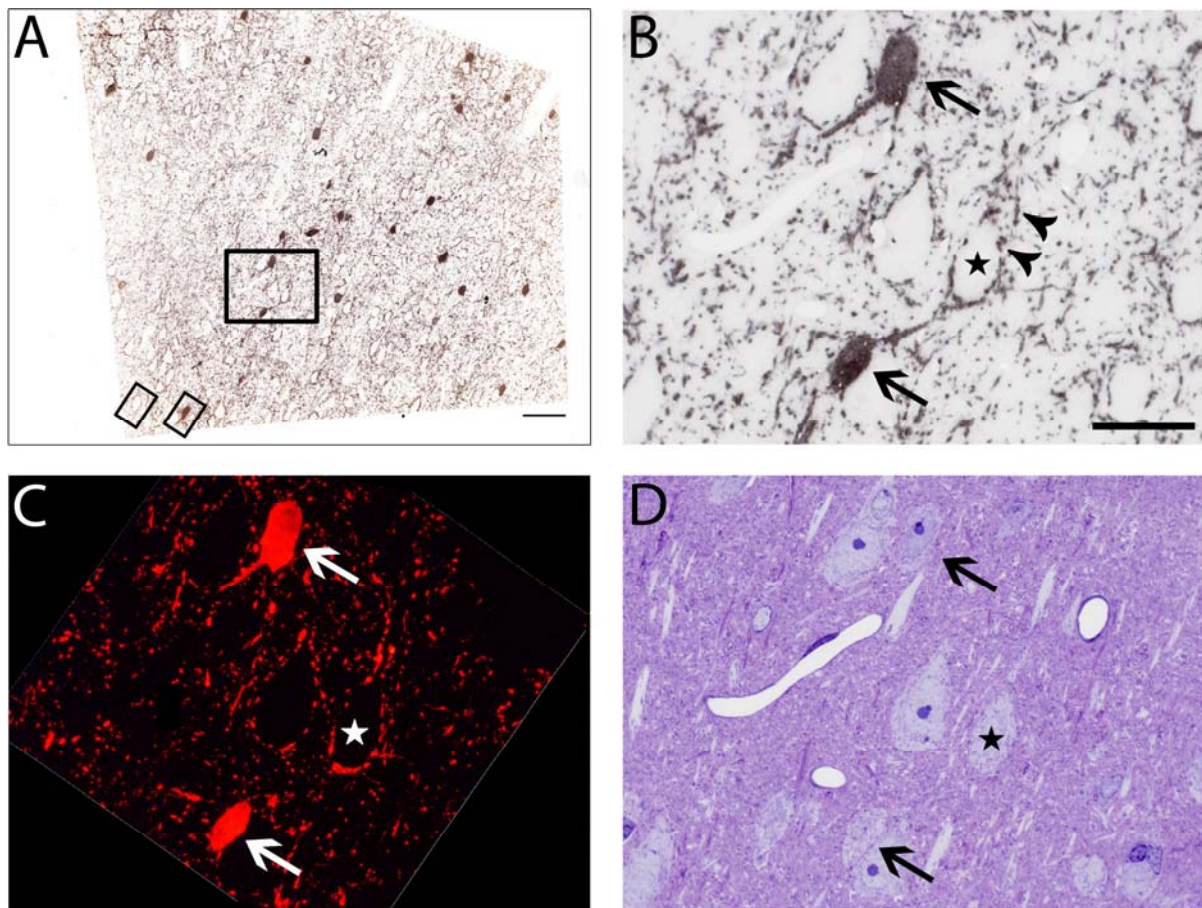


Figure 10: Virtual pre-embedding with CARD (Biotinyl-tyramide at 5 μM). Parvalbumin immunolabeling (compare with figure 2, A and B). **(A)** Post-embedding visualization of biotin by the ABC/DAB procedure on semithin sections (500 nm) of the neocortex displayed a parvalbumin-specific pattern. The larger boxed area is shown at higher magnification in B. Smaller boxed areas are shown at higher magnification in figure 11, A and B. **(B)** Parvalbumin positive neuronal cell bodies (arrows) and elongated and punctate profiles (arrowheads) were distinctly labeled. **(C)** On an adjacent section, biotin was visualized using Alexa 568-labeled streptavidin. **(D)** On a toluidine-blue stained adjacent section cell bodies labeled in B and C (arrows) and cell bodies (asterisk) delineated in B and C by parvalbumin-positive axo-somatic terminals can be clearly identified. Scale bars indicate 60 μm (A), 20 μm (B-D).

3.2.7 Digoxigenyl-tyramide and fluoresceine-tyramide CARD are equally suited for virtual pre-embedding

After successful VirP-labeling with BT-CARD, the use of other hapten-tyramides and CARD was explored. Virtual pre-embedding was performed using digoxigenyl-tyramide and fluoresceine-tyramide at the previously determined optimal concentrations (2 μM and 10 μM ; compare Fig. 7). In semithin cortical sections, labeling of the haptens yielded a DAB staining pattern characteristic of parvalbumin immunoreactivity (compare Figure 5, A-C).

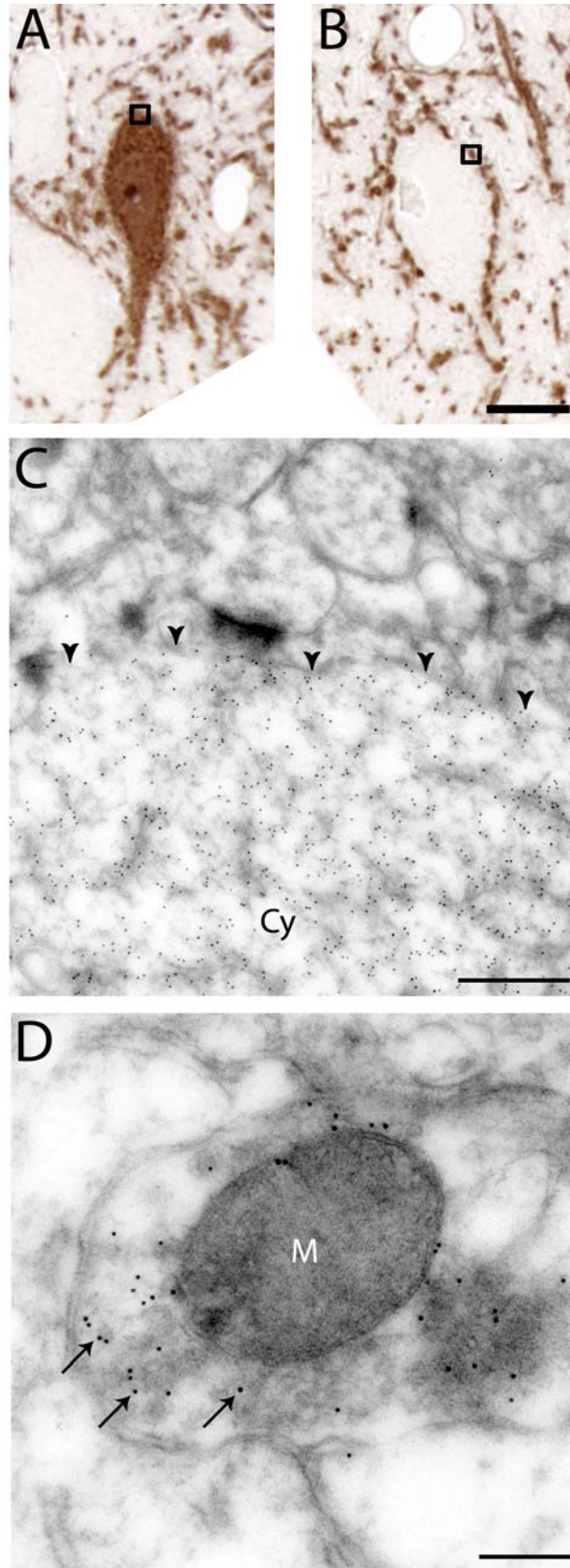


Figure 11: Virtual pre-embedding with CARD (Biotinyl-tyramide at 5 μ M). Correlative microscopy of adjacent semithin (A, B) and ultrathin (C, D) neocortical sections labeled for parvalbumin and

visualized with either the ABC/DAB procedure (A, B) or colloidal gold (C, D). Areas shown in A and B are indicated by the smaller boxes in figure 10 A. In semithin sections, strongly labeled neuronal cell bodies (A) and punctate and elongated profiles (B) were distinctly displayed. (C) On an adjacent ultrathin section, 10 nm colloidal gold particles densely labeled the biotin moieties in the cytoplasm of the same neuron as shown in A. The cell border is indicated by arrowheads. (D) Similarly, the putative axosomatic terminal framed in B displayed a robust 10 nm colloidal gold labeling (arrows). Scale bars indicate 30 μ M (A), 500 nm (B), 200 nm (C). Cy=cytoplasm, M=mitochondrion

When compared with BT, labeling with FT resulted in a less intensely colored brownish reaction product (Figure 12, A-B). Neuronal cell bodies and processes labeled for DT exhibited a strong and dark brown staining comparable with BT (Figure 13, A-C; compare Figure 10, B).

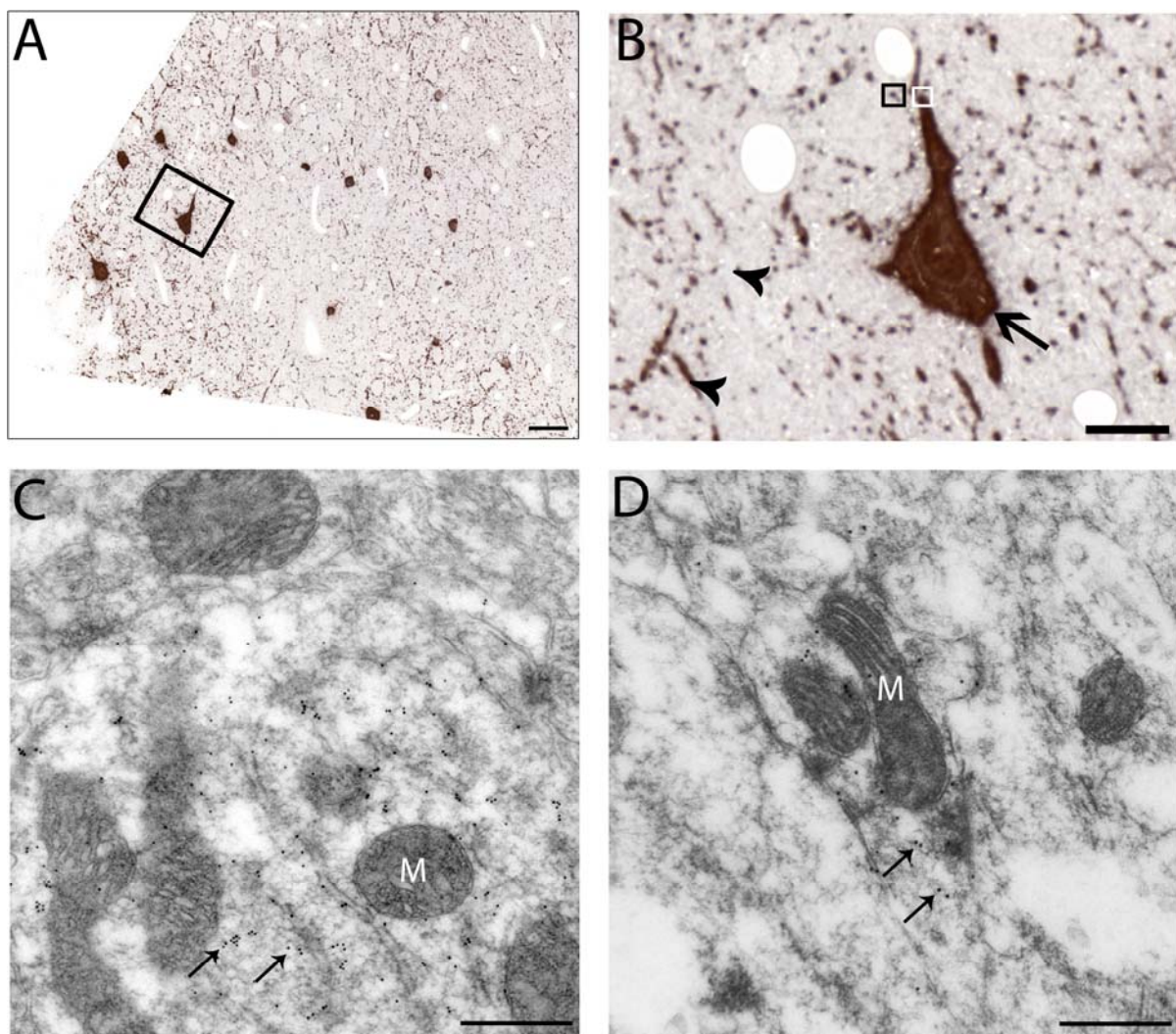


Figure 12: Virtual pre-embedding with CARD and digoxigenyl-tyramide at 2 μ M. Parvalbumin immunolabeling. (A) Postembedding visualization of digoxigenin by the ABC/DAB technique in semithin cortical sections revealed a similar immunoreactivity as observed for the hapten biotin (compare figure 10). The boxed area is shown at higher magnification in B. (B) Punctate and elongated parvalbumin-positive profiles (arrowheads) were clearly visible. (C) On an adjacent ultrathin section, 10 nm colloidal gold particles (arrows) densely labeled the digoxigenin moieties in the cytoplasm of the same neuron as shown in B (white box). (D) Similarly, the terminal marked in B

(black box) displayed a robust 10 nm colloidal gold labeling (arrows). Compare the labeling intensity in Fig. 11. Scale bars indicate 60 μm (A), 30 μm (B), 500 nm (C), 200 nm (D). M=mitochondrion

In ultrathin sections, colloidal gold labeling for digoxigenin (Figure 12, C-D) and fluoresceine (Figure 13, D-E) was strong and specifically restricted to cell bodies and terminals of parvalbumin-containing interneurons.

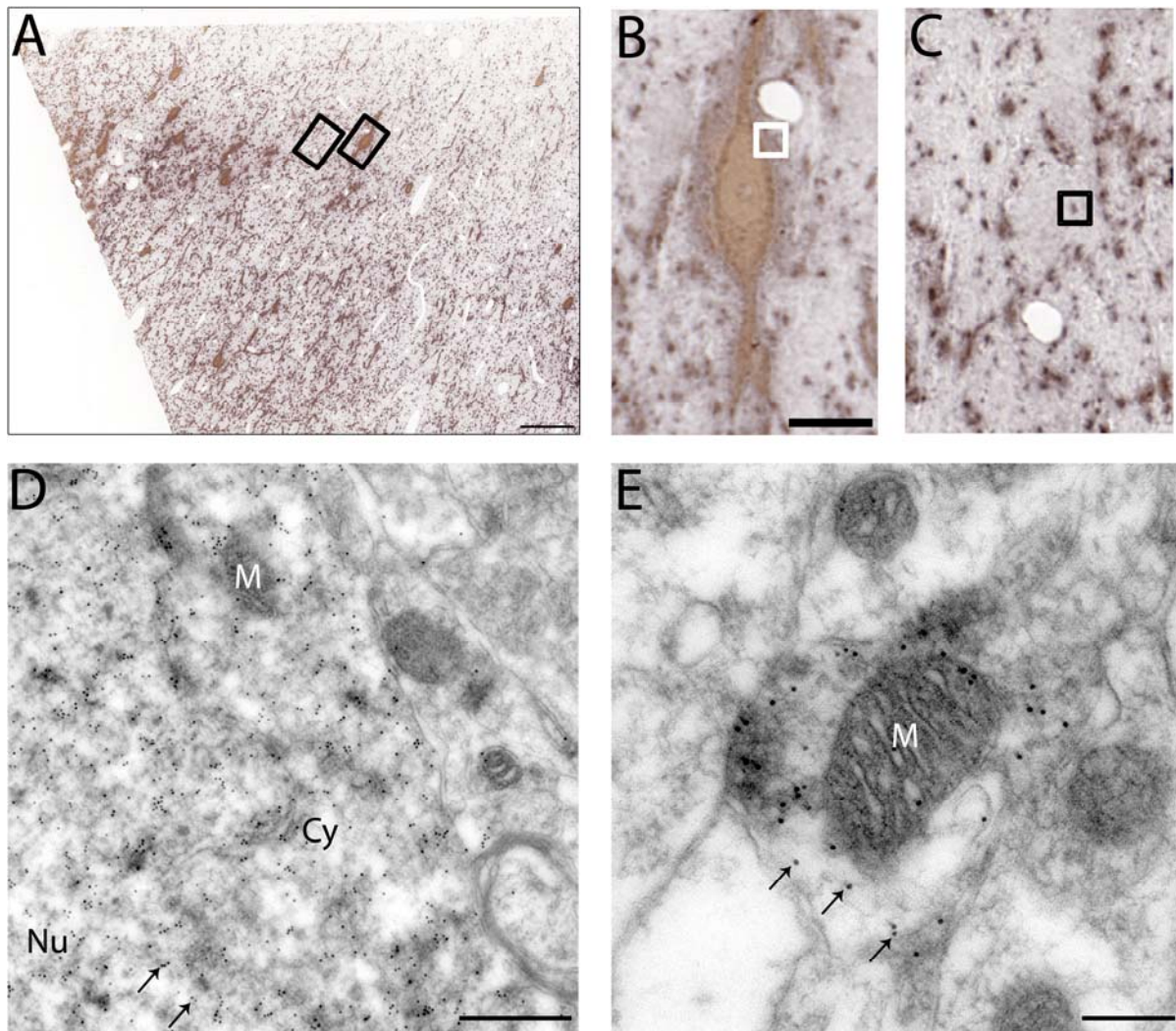


Figure 13: Virtual pre-embedding with CARD and fluoresceine-tyramide at 10 μM . Parvalbumin immunolabeling. (A) Post-embedding DAB signal in semithin cortical sections appeared brownish in cell bodies when compared to the signal obtained for biotin and digoxigenin, but with a similar pattern of immunoreactivity. Boxed areas are shown at higher magnification in B and C: Cell body labeling (B) and an axo-somatic terminal (C). (D) On an adjacent ultrathin section, 10 nm colloidal gold particles (arrows) densely labeled the fluoresceine moieties in the cytoplasm of the same neuron as shown in B. (E) The axosomatic terminal marked in C displayed a strong 10 nm colloidal gold labeling (arrows). Compare the labeling intensity in Figs. 11 and 12. Bars indicate 60 μm (A), 30 μm (B), 500 nm (C), 200 nm (D)

3.2.8 Virtual pre-embedding with tetramethylrhodamine-tyramide

CARD is well suited for correlative microscopy and double labeling

To assess the feasibility of virtual pre-embedding for correlative fluorescence and electron microscopy and double labeling, VirP was conducted with fluorescent tetramethylrhodamine-tyramide (TMRT) to detect parvalbumin. This approach was combined with immunogold-silver-enhancement (IGE) double labeling, displaying glutamic acid decarboxylase (GAD) immunoreactivity, known to be co-localized with parvalbumin in a subset of cortical interneurons.

Prior to embedding, neurons containing silver particles were localized by bright field microscopy (Figure 14, A). Double-labeled neurons in the same section were subsequently identified by fluorescence microscopy (Figure 14, B). After embedding, tetramethylrhodamine immunoreactivity visualized on semithin sections by the ABC/DAB procedure was clearly distinguishable from black silver particles and correlated very well with the previously obtained whole mount fluorescence signal (Figure 14, B-D).

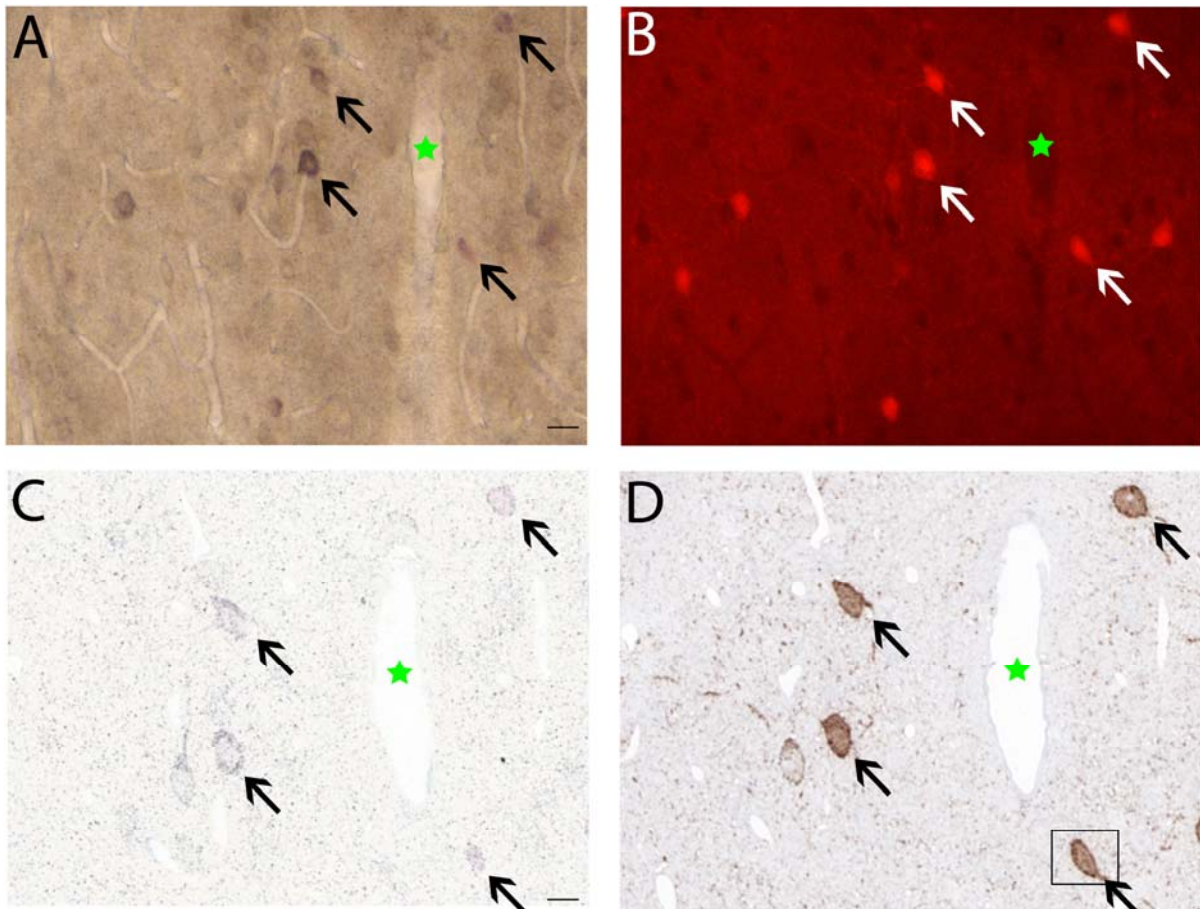


Figure 14: Virtual pre-embedding with CARD and tetramethylrhodamine-tyramide (TMRT) at 10 μ M in combination with immunogold-silver-enhancement (IGE). Parvalbumin was labeled with virtual pre-

embedding and glutamic acid decarboxylase (GAD67) with IGE. **(A)** By light microscopic examination (reversible aqueous mounting) before embedding, neurons positive for silver particles were readily visible in rat neocortex (arrows). **(B)** Double labeling of neurons was confirmed by fluorescence of deposited tetramethylrhodamine (arrows). **(C)** The same neurons positive for silver particles as in A (arrows) were clearly visible after embedding in araldite in semithin sections. **(D)** On an adjacent semithin section, visualization of tetramethylrhodamine by DAB corresponded to the image obtained by fluorescence in B (arrows). The boxed cell is shown at higher magnification in figure 15, A. Asterisks mark the identical blood vessel. Scale bars indicate 30 μ M (A,B), 20 μ M (C,D)

In ultrathin sections, colloidal gold labeling for tetramethylrhodamine was dense and highly specific (Figure 15, C and D; compare Figures 11-13). Both particulate markers, 10 nm colloidal gold and the silver particles, were readily detected and easily distinguishable from each other and underlying cellular structures (Figure 15, D).

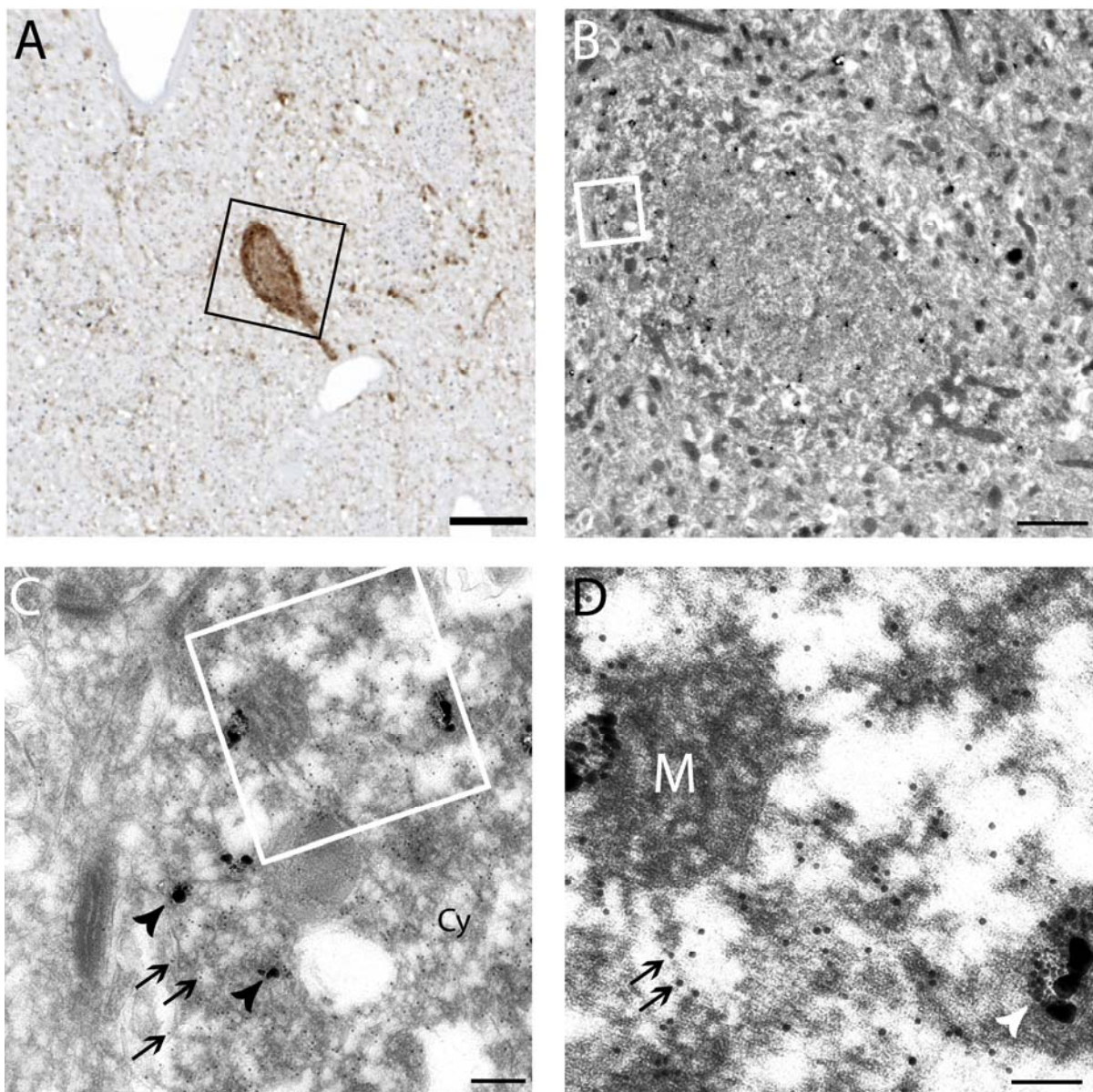


Figure 15: Virtual pre-embedding with CARD and tetramethylrhodamine-tyramide (TMRT) at 10 μ M in combination with immunogold-silver-enhancement. Parvalbumin was labeled with virtual pre-embedding and glutamic acid decarboxylase (GAD67) with the immunogold silver-enhancement

technique (IGE). **(A)** Survey micrograph showing a parvalbumin-positive neuron visualized by the ABC/DAB procedure and identified from fluorescence images recorded before embedding (semithin section; compare figure 14 B and D). **(B)** The cell in A (black box) was identified in an adjacent ultrathin section based on the relative position, size and shape. **(C)** Higher magnification of the white boxed area in B. Irregularly shaped particles from silver enhancement (arrowheads) displaying GAD-like immunoreactivity. Among these, 10 nm colloidal gold particles (arrows), densely labeling the tetramethylrhodamine moieties in the cytoplasm of the neuron, confirmed double labeling. The boxed area is shown at higher magnification in D. **(D)** Both, colloidal gold (arrows) and silver-enhanced particles (arrowhead) were clearly visualized in intensely heavy metal stained areas. Scale bars indicate 10 μm (A), 2 μm (B), 200 nm (C), 100 nm (D). Cy=cytoplasm, (M) mitochondrium

4. Discussion

With the present thesis, it was shown for the first time that haptens provide a stable immunocytochemical affinity system for virtual pre-embedding in rat brain tissue sections. Haptens introduced into the sections by means of haptenylated secondary antibodies allowed abundant antigens to be detected. Haptens deposited by hapten-amplification (i.e. CARD) provided a highly sensitive and specific signal and this technique can be used as a novel tool for double labeling with IGE and in correlative fluorescence and electron microscopy.

4.1 Sensitivity of virtual pre-embedding is determined by optimal deposition of haptens in the pre-embedding step

In order to establish a VirP protocol capable of reliably detecting abundant as well as rare antigens, a set of haptens was chosen to serve as stable detection tags. Two substantially different methods of introducing haptens into brain tissue sections were investigated. While the first approach was based on the detection of haptens coupled to primary and secondary antibodies, the second approach included a signal amplification step by using an enzymatically catalyzed hapten deposition system (CARD).

Owing to their chemical stability and thus rather inert characteristics, haptens were expected to be more compatible with resin-embedding and the post-embedding detection process in comparison with protein antigens. Nevertheless, it has to be assumed that a considerable fraction of tissue-bound haptens would still not be available for antibody labeling after embedding: On the one hand, epitopes can be labeled only at the surface of resin sections. On the other hand, after embedding in epoxy resins a cross-linking between resin components and haptens may occur, even if less pronounced when compared with proteins antigens. Therefore, a critical amount of chemically unmodified hapten available at the surface of thin sections is required for successful post-embedding labeling. This minimum threshold of section-bound hapten after embedding, however, is correlated with the amount of deposited hapten prior to embedding: The more haptens are deposited in the tissue prior to embedding, the higher the probability that enough haptens are available for post-embedding labeling. Apparently, this threshold was not reached when haptenylated primary antibodies were used. Although haptens coupled to primary antibodies were clearly visualized in cryostat and vibratome sections for light microscopy, after

embedding in araldite no hapten-specific immunoreactivity could be detected. This finding may be explained by a general immunocytochemical principle favoring so called indirect labeling methods. Using a labeled secondary antibody, e.g. carrying an enzyme or fluorophore, generally results in a marked increase in sensitivity when compared to the direct approach with a labeled primary antibody.⁵⁸ Multiple secondary antibodies are able to bind to one primary antibody, thereby increasing the amount of labeling and subsequently signal intensity.

Other factors may also have influenced the sensitivity of the approach. When using haptenylated antibodies, the amount of tissue-bound hapten depends on at least four more major premises: the relative amount of antigen expressed, its accessibility with pre-embedding techniques, the affinity of the antibody to the antigen, and the efficiency of haptenylation, i.e. the number of hapten molecules conjugated to one immunoglobulin. By using serotonergic projection neurons of the dorsal raphe as a model system, with 5-HT an abundant rather than a rare antigen was chosen to avoid unsuccessful labeling due to limited availability. The use of vibratome sections, which tend to be less permeable for antibodies than cryosections, may account for some loss in sensitivity, but it is indispensable, as they offer improved ultrastructural morphology. While the affinity of an antibody can usually not be increased, the efficiency of haptenylation can be optimized. A well-characterized haptenylation-method was used and successful haptenylation and anti-hapten immunoreactivity were verified. Taken together, the use of haptenylated primary antibodies for VirP shows little prospect for success.

By contrast, with biotinylated secondary antibodies a comparatively weak but clearly specific and reproducible VirP signal was obtained. As expected, the indirect labeling approach led to the deposition of increased amounts of biotin, thus allowing a successful hapten labeling after embedding. Again, the target antigen (parvalbumin) was strongly expressed, in this case in GABAergic interneurons. Considering the still rather weak signal obtained with the indirect labeling approach, it seems likely, however, that under these conditions VirP is restricted to the detection of abundant antigens. This approach would therefore be ideally suited for tracing studies, since tracers are present in neurons at high concentrations. With this application, virtual pre-embedding with haptenylated secondary antibodies may be a useful tool for double or even multiple labeling tracing studies.

⁵⁸ (Griffiths, G et al. 1993, p. 261ff)

Based on these results obtained with haptenylated antibodies, it could be anticipated that the use of an enzyme-based amplification system, namely CARD, would further increase the amount of hapten molecules available for post-embedding detection. However, the detection of rare antigens may require optimizing the conditions for deposition of hapten-tyramides in order to achieve maximum sensitivity. Therefore, it was investigated first, whether a purification of the hapten-tyramides, that is removal of potentially remaining activated hapten-ester or tyramine after synthesis, would prove beneficial for hapten deposition. Unexpectedly, unpurified BT led to higher enzyme activity than purified BT and unpurified tyramide-conjugates were used in all CARD-based experiments. Interestingly, a study using CARD for in-situ hybridization⁵⁹ similarly favored the use of the unpurified reagent. Next, as optimal deposition of hapten-tyramides is concentration-dependent, the optimal concentrations were determined in an ELISA model system. The investigation of individual hapten-tyramides led to unexpected concentration-dependent enzyme-activities. With tetramethylrhodamine-tyramide and Texas-Red-tyramide, moderately sharp peaks of activity with a maximum at 4 μM (range 2 – 10 μM) were observed. Digoxigenyl-tyramide with a very sharp peak at 3 μM and biotinyl-tyramide with a broader range of optimal activity between 5 – 12 μM without an observable peak clearly showed different characteristics. All mentioned tyramide-conjugates led to a decrease in signal strength with increasing concentrations with the exception of FT, which displayed a peak with a maximum at 4 μM followed by a slight increase at very high concentrations. However, these results are in good agreement with the literature (Table 4) and point out that, depending on the type of hapten, the chemical behavior of the hapten-tyramides as peroxidase-substrates is obviously significantly different. The differences in activity observed in the ELISA assay were also evident on brain sections (compare Fig. 8), where BT at 5 μM was superior with regard to the signal-to-noise ratio when compared to 1 and 20 μM . In consequence, optimal concentration ranges have to be individually determined for all new hapten-tyramide conjugates before their use in immunocytochemistry.

⁵⁹ (Hopman, AH et al. 1998)

	Optimal concentration range as determined in this thesis	Concentrations used in the literature
BT	5 - 12	3.5 ^a
DT	0,5 - 5	3 ^a
FT	2 - 10	8.1 ^a , 1-5 ^{b,d} , 7,5 ^c

Table 4 Concentrations of hapten-tyramides (μM) for use with immunocytochemistry as determined in this study and compared with the available literature. a) (Hopman, AH et al. 1998) b) (Raap, AK et al. 1995) c) (van Gijlswijk, RP et al. 1997), d) (Speel, EJ et al. 1997).

Initial VirP experiments using BT and P-SA with vibratome sections led to the observation that the signal was restricted to the surface of the sections. Apparently, haptens were not deposited beyond a depth of several microns during the pre-embedding step. Penetration studies with cross-sectioned slices comparing P-SA and ELITE ABC revealed that this restriction was only observed when P-SA was used. For light microscopic immunocytochemistry, P-SA offers an improved signal-to-noise ratio when compared to ABC. However, this improved signal-to-noise ratio of P-SA may not entirely depend on low background labeling, but also on a restricted penetration of P-SA resulting in a background labeling comparable to that obtained when using thinner sections. Thus, P-SA cannot be used when optimal penetration of haptens or visualization agents is required. ELITE ABC, by contrast, was successfully used with all synthesized hapten-tyramide conjugates and yielded comparatively strong labeling.

4.2 Single labeling with virtual pre-embedding offers considerable advantages over routinely used pre-embedding techniques

Owing to the high electron density of colloidal gold particles, the immunosignal achieved with VirP was easily identifiable and distinguishable from underlying heavy metal stained cellular structures and organelles. The preservation of morphological information in the presence of intense specific labeling paired with the easy-to-use and reproducible HRP-based procedure, offers distinct advantages when compared to widely used standard pre-embedding techniques.

Peroxidase/DAB labeling, though easily performed and sensitive, clearly suffers from obscuring ultrastructural details due to the diffusibility of the reaction product within membranous compartments. Spreading of the reaction product leads to an inevitable loss of resolution within the respective compartment, e.g. a dendritic spine. A transformation of the DAB signal into a

particulate signal with the help of silver intensification is possible⁶⁰, but cannot compensate for the preceding spreading of the signal and hence does not improve resolution. Moreover, hapten-tyramide radicals created by CARD are likely to spread less when compared to classical DAB techniques, since they very quickly react with molecules in the vicinity of the antigen site. By increasing the viscosity of the CARD buffer, diffusibility of hapten tyramides could effectively be further decreased, thereby increasing resolution, though at the expense of the amplification rate (data not shown). Hence, resolution of CARD VirP can be fine-tuned according to the requirements with respect to precision of localization and sensitivity.

By contrast, IGE, the second widely used pre-embedding technique using small gold particles of 1 to 1.4 nm size in combination with silver enhancement⁶¹, allows for a precise localization of the antigen within the limit of the created silver particle size. In comparison to enzyme-based methods, however, the IGE signal may often be considered less sensitive and less reproducible.

Compared with these standard procedures, CARD VirP offers an easy-to-use and highly amplifying labeling technique with good penetration properties in pre-embedding labeling. It does, however, involve an additional post-embedding step to visualize the deposited hapten, thus increasing the amount of time needed to complete labeling experiments. Also, additional expertise in post-embedding labeling is required.

4.3 Double labeling with virtual pre-embedding offers considerable advantages over routinely used pre-embedding techniques

Pre-embedding methods are of crucial importance for tracing studies used to investigate cerebral connectivity. Anterograde and retrograde tracers are transported along axons *in vivo* and thereby help to identify neural circuitries. Frequently, identification of more than one tracer or neurotransmitter requires double labeling techniques. Therefore, novel pre-embedding techniques need to be compatible with existing pre-embedding techniques to allow double labeling. It was shown that CARD-based VirP could be combined with IGE in a double labeling approach, visualizing GAD67 (IGE) simultaneously with parvalbumin (VirP) in GABAergic interneurons. With both techniques, antigens were labeled by clearly distinguishable particulate markers, i.e. silver-enhanced gold particles and colloidal gold particles. Ultrastructural details

⁶⁰ (Smiley, JF et al. 1993)

⁶¹ (Lackie, PM et al. 1985; Chan, J et al. 1990; Dulhunty, AF et al. 1993)

were not obscured and allowed for precise localization of the signal. By contrast, conventional pre-embedding double labeling approaches suffer from certain limitations. As described above, the application of DAB as a peroxidase substrate is limited by obscured ultrastructural details. Alternative substances, namely benzidine dihydrochloride or tetramethylbenzidine, yield large and wide crystals, which may hinder the visualization of small structures, e.g. neuronal processes.⁶² Also, if two peroxidase-based approaches are combined, the specificity of both labelings must be ensured. Double labeling with autoradiographic approaches, at last, may be impractical due to long exposure times and low resolution.⁶³

In conclusion, VirP seems to be well suited for double labeling approaches in combination with IGE. It should be noted, however, that this combination also has some restrictions. With VirP, an additional post-embedding step has to be performed, whilst IGE needs more careful handling of the procedure. Therefore, some experience has to be gathered in order to successfully and reliably combine the two techniques. Since for methodological reasons abundant antigens were used to establish VirP, it still has to be shown whether rare antigens could also be reliably visualized.

4.4 Virtual pre-embedding is an easy-to-use and inexpensive alternative for correlative microscopy studies

Correlative microscopy studies have become increasingly important in immunocytochemistry. The analysis of the highly complex brain tissue requires a signal transfer from light microscopy, e.g. live-cell-imaging, to fine structural analysis with electron microscopy.

The most widely used approach in correlative microscopy in neuroscience is the correlation of light and electron microscopy (CLEM). It allows for the screening of cellular structures and processes at low magnifications, which can then be further analyzed on an ultrastructural level after embedding. In this thesis, tetramethylrhodamine as a fluorescent hapten-tyramide-conjugate (TMRT) was used with VirP for the correlation of fluorescence and electron microscopy (Figs. 14 and 15). Parvalbumin-positive neurons in rat brain cerebral cortex were successfully fluorescence-screened and documented, followed by the identification of the same cells on the ultrastructural level. Apparently, the amount of deposited TMRT was sufficiently high to provide

⁶² (Carson, KA et al. 1982; Levey, AI et al. 1986)

⁶³ (Pickel, VM et al. 1986)

both a bright fluorescent signal prior to embedding and a successful post-embedding visualization yielding a dense colloidal gold signal. CARD VirP combines the advantages of individual immunocytochemical techniques, e.g. fluorescence microscopy, with an enzymatic amplification of the signal.

Other techniques for the correlation of fluorescence and electron microscopy exist. The FluoroNanogold[®] system employs a fluorophore and an ultrasmall gold particle, both tagged to the same antibody. However, the published studies were mostly restricted to cultured cells⁶⁴. Recently, FluoroNanogold[®] was also used for the labeling of antigens in vibratome sections from drosophila muscle with a reported penetration depth of 10 nm.⁶⁵ However, it still remains unclear whether similar results could be achieved with membrane-rich brain tissue. Yet another approach is used in photoconversion, utilizing the chemical oxidation of DAB by fluorophores exposed to strong UV light. Apart from studies with cultured cells, only a few studies used photoconversion with brain tissue sections. While some studies required a 12-month incubation period for the fluorescent dye⁶⁶, in other cases the fluorophore was injected.⁶⁷ Moreover, the area recruited for photoconversion is relatively small and the procedure is time consuming and requires toxic reagents.⁶⁸ Thus, the applicability of photoconversion following immunolabeling with fluorophores in CNS tissue sections is limited. Another tool for correlative microscopy are quantum dots of different size, which have been successfully used for correlative multilabeling in cultured cells and mouse cerebellum.⁶⁹ They provide a bright fluorescence signal but are only moderately electron dense. However, with tissue sections, it may be necessary that staining with heavy metals must be omitted to allow the identification of small quantum dots. The resulting contrast impairment leads to a loss of ultrastructural information. Furthermore, due to the fluorescent characteristics of quantum dots, special and expensive filter sets are necessary.

In conclusion, CARD-based virtual pre-embedding offers a useful and inexpensive alternative for correlative light and electron microscopy studies of the CNS.

⁶⁴ (Robinson, JM et al. 1997; Takizawa, T et al. 1998; Robinson, JM et al. 2000)

⁶⁵ (Jiao, W et al. 2010)

⁶⁶ (Singleton, CD et al. 1996)

⁶⁷ (Nikonenko, I et al. 2005; Toni, N et al. 2007)

⁶⁸ (Singleton, CD et al. 1996)

⁶⁹ (Giepmans, BN et al. 2005)

4.5 Virtual pre-embedding may provide a useful new tool for future immunocytochemical studies of the CNS

As correlative light and electron microscopy is a technique with increasing popularity, VirP will be of interest especially in those approaches requiring a significant amplification of the signal systems. Since the technique does not require special equipment or chemicals, it is likely to be easily implemented in laboratory routine. Furthermore, it was shown that the VirP-signal was not significantly affected by the immunogold silver enhancement technique. This suggests that VirP is likely to be suited for a combination with immunogold silver enhancement in double labeling experiments, e.g. the labeling of two tracers or the combination of a tracer and a synaptic antigen. Provided that both signals are visualized by fluorescence microscopy prior to embedding, double correlative analysis would also be possible and potential synaptic contacts could be easily identified prior to embedding. With confocal microscopy, also spatial information about the labeled structures could be gained, facilitating not only the identification of rare synaptic connections prior to embedding, but also allowing the retrieval of labeled structures during thin sectioning.

Some synaptic proteins, e.g. monoamine transporters, are highly expressed in neuronal processes and may be suited for post-embedding visualization also in epoxy-resins. As VirP already includes a post-embedding step, an additional post-embedding labeling may be performed, allowing triple labeling.

5 Conclusion

Virtual pre-embedding labeling with haptens provides a stable immunocytochemical affinity system in CNS tissue sections. The most promising results were obtained with an enzymatically catalyzed amplification of hapten-tyramide conjugates (CARD). CARD virtual pre-embedding was successfully introduced as an alternative method for double labeling with immunogold-enhancement and correlative fluorescence and electron microscopy, suggesting that VirP will provide a useful tool for future immunocytochemical studies of CNS function.

6 Summary

In neuroscience, it is important to localize antigens to subcellular structures. For this purpose, electron microscopic immunocytochemical methods are used. Immunocytochemical labeling for electron microscopy is performed either *prior to* embedding the tissue in artificial resin, by so called pre-embedding techniques, or *after* embedding, by so called post-embedding techniques. For methodological reasons, e.g. possible quantification of the signal, post-embedding approaches are preferred. However, many antigens are not available for post-embedding labeling after the embedding step. Pre-embedding techniques not only provide an alternative, but are necessary for certain immunocytochemical approaches: on one hand for tracing studies, where synaptic connections between cell types of different brain areas must be unequivocally identified in double (or multiple) labeling studies. On the other hand for correlative light and electron microscopy, a synergistic approach, which allows for the pre-examination of large tissue areas and identification of regions of interest (ROI) by fluorescence microscopy screening, followed by analysis of the ultrastructure of the ROIs by electron microscopy. Routinely used pre-embedding techniques, however, such as the combination of peroxidase and benzidine-compounds or the immunogold-silver-enhancement method (IGE), suffer from distinctive drawbacks. Benzidine-peroxidase techniques allow only limited fine localization owing to the diffusibility of the reaction products, while IGE may be considered less sensitive and reproducible. In the present thesis, a novel method utilizing haptens, i.e. small and chemically inert molecules like biotin, combining the pre- and postembedding techniques was tested as an alternative electron microscopic labeling technique in rat brain tissue sections. In the pre-embedding step, antigens were indirectly labeled with haptens. The haptens were introduced into the tissue either coupled to antibodies or by use of a peroxidase-based hapten amplification system, i.e. catalyzed reporter deposition (CARD). After embedding, instead of the original antigen, the haptens introduced were labeled in a post-embedding step. This approach was termed “virtual pre-embedding” (VirP) in this work.

While hapten-coupled primary antibodies yielded no signal with virtual pre-embedding, with hapten-coupled secondary antibodies, a comparatively weak but clearly specific and reproducible VirP signal was obtained. The most promising results were attained with the CARD-based deposition of haptens offering considerable advantages over routinely used pre-embedding methods: This approach yielded a sensitive, specific and reproducible signal with excellent contrast for four different haptens as reporter molecules. Moreover, it was shown that

CARD VirP was suited for double-labeling with IGE and for correlative fluorescence and electron microscopy using a fluorescent hapten.

In conclusion, CARD virtual pre-embedding was successfully introduced as an alternative method for pre-embedding labeling, double labeling studies and correlative fluorescence and electron microscopy. This suggests that virtual pre-embedding will provide a useful tool for future immunocytochemical studies of brain function.

7 Zusammenfassung

Die präzise subzelluläre Lokalisation von Antigenen ist in den Neurowissenschaften von großer Bedeutung. Zu diesem Zweck werden elektronenmikroskopisch-immuncytochemische Methoden eingesetzt. Die Markierung des Gewebes mit Antikörpern wird für die Elektronenmikroskopie entweder vor der Einbettung des Gewebes in Kunstharz, im so genannten „pre-embedding“-Verfahren, oder nach der Einbettung, im so genannten „post-embedding“-Verfahren, durchgeführt. Im Unterschied zum „pre-embedding“-Verfahren sind im „post-embedding“-Verfahren alle zellulären Kompartimente gleichermaßen zugänglich und die Markierungen quantifizierbar. Da jedoch viele Antigene nach der Einbettung im „post-embedding“-Verfahren mit den zur Verfügung stehenden Antikörpern nicht nachweisbar sind, werden häufig alternativ „pre-embedding“-Methoden eingesetzt. Darüber hinaus sind „pre-embedding“-Verfahren essentiell für tracing Studien, mit deren Hilfe synaptische Verbindungen zwischen bestimmten Hirnarealen unter Verwendung immuncytochemischer Doppel- (oder Mehrfach)markierungen identifiziert werden und für die Korrelation von Licht- und Elektronenmikroskopie. Hierbei handelt es sich um einen synergistischen Ansatz, welcher es erlaubt, mittels Fluoreszenzmikroskopie großflächig Gewebeanteile zu untersuchen und dann kleinere Regionen von Interesse zu definieren, deren Ultrastruktur nachfolgend mittels Elektronenmikroskopie untersucht werden kann. Für diese Zwecke haben sich im wesentlichen zwei „pre-embedding“-Techniken bewährt, zum einen die Kombination des Enzyms Peroxidase mit Benzidinderivaten und zum anderen die Immunogold-Silberverstärkung (IGE). Peroxidase-Benzidin-Techniken sind durch eine eingeschränkte Feinlokalisierung gekennzeichnet, während die Sensitivität des IGE-Verfahrens bei relativ schwach exprimierten Antigenen zum limitierenden Faktor werden kann. In der vorliegenden Arbeit wurde ein neuer Ansatz untersucht, bei dem durch die Kombination von „pre-“, und „post-embedding“-Techniken unter Verwendung von Haptenen elektronenmikroskopische Markierungen an Hirnschnitten der Ratte durchgeführt wurden. Im „pre-embedding“-Schritt wurden dabei Antigene mit Haptenen markiert. Die Haptene wurden entweder an Antikörper gekoppelt oder durch ein Peroxidase-basiertes Hapten-Amplifikationssystem (CARD, **C**Alyzed **R**eporter **D**eposition) in das Gewebe eingebracht. Nach der Einbettung wurden in einem „post-embedding“- Schritt nun die Haptene und nicht das ursprüngliche Antigen markiert. Dieser Ansatz wurde in der vorliegenden Arbeit „virtuelles pre-embedding“ (VirP) genannt.

Während mittels an Primärantikörper gekoppelter Haptene kein VirP-Signal erzielt werden konnte, war mit an Sekundärantikörper gekoppelten Haptenen ein verhältnismäßig schwaches,

jedoch klar spezifisches und reproduzierbares Signal nachweisbar. Die vielversprechendsten Ergebnisse konnten mit der CARD-basierten Verstärkung der Haptenablagerung erzielt werden. Diese Methode verbindet eine durch die Signalverstärkung erzielte hohe Sensitivität mit den Vorteilen eines partikulären Markersystems. Das erzielte spezifische Signal zeichnete sich bei allen vier untersuchten Haptenen durch hohe Sensitivität, gute Reproduzierbarkeit und leichte Darstellbarkeit aus. VirP eignet sich zudem für Doppelmarkierungen in Kombination mit IGE und für korrelative Fluoreszenz- und Elektronenmikroskopie unter Nutzung eines fluoreszierenden Haptens.

Zusammenfassend wurde in der vorliegenden Arbeit CARD-basiertes VirP erfolgreich als alternative Methode für herkömmliche pre-embedding Markierungen, für Doppelmarkierungsstudien und die Korrelation von Fluoreszenz- und Elektronenmikroskopie angewendet. Diese Ergebnisse legen nahe, dass VirP sich als eine neue, breit anwendbare Methode für die Untersuchung von Gehirnstruktur und -funktion etablieren könnte.

8 References

- Adams, J. C. (1992). "Biotin amplification of biotin and horseradish peroxidase signals in histochemical stains." J Histochem Cytochem **40**(10): 1457-63.
- Afzelius, B. A. and A. B. Maunsbach (2004). "Biological ultrastructure research; the first 50 years." Tissue Cell **36**(2): 83-94.
- Asan, E. and D. Drenckhahn (2008). "State-of-the-art technologies, current opinions and developments, and novel findings: news from the field of histochemistry and cell biology." Histochem Cell Biol **130**(6): 1205-51.
- Baschong, W. and Y. D. Stierhof (1998). "Preparation, use, and enlargement of ultrasmall gold particles in immunoelectron microscopy." Microsc Res Tech **42**(1): 66-79.
- Bayani, J. and J. A. Squire (2004). "Fluorescence in situ Hybridization (FISH)." Curr Protoc Cell Biol **Chapter 22**: Unit 22 4.
- Behringer, D. M., K. H. Meyer and R. W. Veh (1991). "Antibodies against neuroactive amino acids and neuropeptides. II. Simultaneous immunoenzymatic double staining with labeled primary antibodies of the same species and a combination of the ABC method and the hapten-anti-hapten bridge (HAB) technique." J Histochem Cytochem **39**(6): 761-70.
- Bobrow, M. N., T. D. Harris, K. J. Shaughnessy and G. J. Litt (1989). "Catalyzed reporter deposition, a novel method of signal amplification. Application to immunoassays." J Immunol Methods **125**(1-2): 279-85.
- Bobrow, M. N., K. J. Shaughnessy and G. J. Litt (1991). "Catalyzed reporter deposition, a novel method of signal amplification. II. Application to membrane immunoassays." J Immunol Methods **137**(1): 103-12.
- Bratthauer, G. L. (1999). "The avidin-biotin complex (ABC) method and other avidin-biotin binding methods." Methods Mol Biol **115**: 203-14.
- Brorson, S. H., N. Roos and F. Skjorten (1994). "Antibody penetration into LR-White sections." Micron **25**(5): 453-60.
- Bruchez, M., Jr., M. Moronne, P. Gin, S. Weiss and A. P. Alivisatos (1998). "Semiconductor nanocrystals as fluorescent biological labels." Science **281**(5385): 2013-6.
- Buki, A., S. A. Walker, J. R. Stone and J. T. Povlishock (2000). "Novel application of tyramide signal amplification (TSA): ultrastructural visualization of double-labeled immunofluorescent axonal profiles." J Histochem Cytochem **48**(1): 153-61.
- Carlemalm, E., R. Garavito and W. Villiger (1982). "Resin development for electron microscopy and an analysis of embedding at low temperature." J Microsc **126**: 123-143.
- Carson, K. A. and M. M. Mesulam (1982). "Electron microscopic demonstration of neural connections using horseradish peroxidase: a comparison of the tetramethylbenzidine

-
- procedure with seven other histochemical methods." J Histochem Cytochem **30**(5): 425-35.
- Causton, B. E. (1986). Does the embedding chemistry interact with tissue? In: Science of biological specimen preparations. M. Müller, R. Becker, A. Boyle and W. J.J. Chicago, SEM Inc, AMF O'Hare: 209-214.
- Chan, J., C. Aoki and V. M. Pickel (1990). "Optimization of differential immunogold-silver and peroxidase labeling with maintenance of ultrastructure in brain sections before plastic embedding." J Neurosci Methods **33**(2-3): 113-27.
- Chan, W. C. and S. Nie (1998). "Quantum dot bioconjugates for ultrasensitive nonisotopic detection." Science **281**(5385): 2016-8.
- Chao, J., R. DeBiasio, Z. Zhu, K. A. Giuliano and B. F. Schmidt (1996). "Immunofluorescence signal amplification by the enzyme-catalyzed deposition of a fluorescent reporter substrate (CARD)." Cytometry **23**(1): 48-53.
- Chevalier, J., J. Yi, O. Michel and X. M. Tang (1997). "Biotin and digoxigenin as labels for light and electron microscopy in situ hybridization probes: where do we stand?" J Histochem Cytochem **45**(4): 481-91.
- de Haas, R. R., N. P. Verwoerd, M. P. van der Corput, et al. (1996). "The use of peroxidase-mediated deposition of biotin-tyramide in combination with time-resolved fluorescence imaging of europium chelate label in immunohistochemistry and in situ hybridization." J Histochem Cytochem **44**(10): 1091-9.
- Dulhunty, A. F., P. R. Junankar and C. Stanhope (1993). "Immunogold labeling of calcium ATPase in sarcoplasmic reticulum of skeletal muscle: use of 1-nm, 5-nm, and 10-nm gold." J Histochem Cytochem **41**(10): 1459-66.
- Erber, W. N., J. I. Willis and G. J. Hoffman (1997). "An enhanced immunocytochemical method for staining bone marrow trephine sections." J Clin Pathol **50**(5): 389-93.
- Giepmans, B. N. (2008). "Bridging fluorescence microscopy and electron microscopy." Histochem Cell Biol **130**(2): 211-7.
- Giepmans, B. N., T. J. Deerinck, B. L. Smarr, Y. Z. Jones and M. H. Ellisman (2005). "Correlated light and electron microscopic imaging of multiple endogenous proteins using Quantum dots." Nat Methods **2**(10): 743-9.
- Graham, R. C., Jr. and M. J. Karnovsky (1966). "The early stages of absorption of injected horseradish peroxidase in the proximal tubules of mouse kidney: ultrastructural cytochemistry by a new technique." J Histochem Cytochem **14**(4): 291-302.
- Griffin, B. A., S. R. Adams and R. Y. Tsien (1998). "Specific covalent labeling of recombinant protein molecules inside live cells." Science **281**(5374): 269-72.
- Griffiths, G., B. Burke and J. Lucocq (1993). Fine structure immunocytochemistry. Berlin ; New York, Springer-Verlag.

-
- Hainfeld, J. F. and F. R. Furuya (1992). "A 1.4-nm gold cluster covalently attached to antibodies improves immunolabeling." J Histochem Cytochem **40**(2): 177-84.
- Heupel, W. M. and D. Drenckhahn (2009). "Extending the knowledge in histochemistry and cell biology." Histochem Cell Biol.
- Hopman, A. H., F. C. Ramaekers and E. J. Speel (1998). "Rapid synthesis of biotin-, digoxigenin-, trinitrophenyl-, and fluorochrome-labeled tyramides and their application for In situ hybridization using CARD amplification." J Histochem Cytochem **46**(6): 771-7.
- Humbel, B. M., M. D. de Jong, W. H. Muller and A. J. Verkleij (1998). "Pre-embedding immunolabeling for electron microscopy: an evaluation of permeabilization methods and markers." Microsc Res Tech **42**(1): 43-58.
- Hunyady, B., K. Krempels, G. Harta and E. Mezey (1996). "Immunohistochemical signal amplification by catalyzed reporter deposition and its application in double immunostaining." J Histochem Cytochem **44**(12): 1353-62.
- Jiao, W., A. Shupliakov and O. Shupliakov (2010). "A semi-correlative technique for the subcellular localization of proteins in Drosophila synapses." J Neurosci Methods **185**(2): 273-9.
- Lackie, P. M., R. J. Hennessy, G. W. Hacker and J. M. Polak (1985). "Investigation of immunogold-silver staining by electron microscopy." Histochemistry **83**(6): 545-50.
- Lakos, S. and A. I. Basbaum (1986). "Benzidine dihydrochloride as a chromogen for single- and double-label light and electron microscopic immunocytochemical studies." J Histochem Cytochem **34**(8): 1047-56.
- Lee, S. W., S. E. Lee, S. H. Ko, et al. (2005). "Introduction of tyramide signal amplification (TSA) to pre-embedding nanogold-silver staining at the electron microscopic level." J Histochem Cytochem **53**(2): 249-52.
- Levey, A. I., J. P. Bolam, D. B. Rye, et al. (1986). "A light and electron microscopic procedure for sequential double antigen localization using diaminobenzidine and benzidine dihydrochloride." J Histochem Cytochem **34**(11): 1449-57.
- Li, C. Y., S. C. Ziesmer and O. Lazcano-Villareal (1987). "Use of azide and hydrogen peroxide as an inhibitor for endogenous peroxidase in the immunoperoxidase method." J Histochem Cytochem **35**(12): 1457-60.
- Lubke, J. (1993). "Photoconversion of diaminobenzidine with different fluorescent neuronal markers into a light and electron microscopic dense reaction product." Microsc Res Tech **24**(1): 2-14.

-
- Lujan, R., J. D. Roberts, R. Shigemoto, H. Ohishi and P. Somogyi (1997). "Differential plasma membrane distribution of metabotropic glutamate receptors mGluR1 alpha, mGluR2 and mGluR5, relative to neurotransmitter release sites." J Chem Neuroanat **13**(4): 219-41.
- Martin, B. R., B. N. Giepmans, S. R. Adams and R. Y. Tsien (2005). "Mammalian cell-based optimization of the biarsenical-binding tetracysteine motif for improved fluorescence and affinity." Nat Biotechnol **23**(10): 1308-14.
- Mayer, G. and M. Bendayan (1997). "Biotinyl-tyramide: a novel approach for electron microscopic immunocytochemistry." J Histochem Cytochem **45**(11): 1449-54.
- Mayer, G. and M. Bendayan (1999). "Immunogold signal amplification: Application of the CARD approach to electron microscopy." J Histochem Cytochem **47**(4): 421-30.
- Mayer, G. and M. Bendayan (2001). "Amplification methods for the immunolocalization of rare molecules in cells and tissues." Prog Histochem Cytochem **36**(1): 3-85.
- Mayer, G., R. D. Leone, J. F. Hainfeld and M. Bendayan (2000). "Introduction of a novel HRP substrate-Nanogold probe for signal amplification in immunocytochemistry." J Histochem Cytochem **48**(4): 461-70.
- McDonald, K. L. and M. Auer (2006). "High-pressure freezing, cellular tomography, and structural cell biology." Biotechniques **41**(2): 137, 139, 141 passim.
- Meiblitzer-Ruppitsch, C., M. Vetterlein, H. Stangl, et al. (2008). "Electron microscopic visualization of fluorescent signals in cellular compartments and organelles by means of DAB-photoconversion." Histochem Cell Biol **130**(2): 407-19.
- Merz, H., R. Malisius, S. Mannweiler, et al. (1995). "ImmunoMax. A maximized immunohistochemical method for the retrieval and enhancement of hidden antigens." Lab Invest **73**(1): 149-56.
- Michalet, X., F. F. Pinaud, L. A. Bentolila, et al. (2005). "Quantum dots for live cells, in vivo imaging, and diagnostics." Science **307**(5709): 538-44.
- Mironov, A. A. and G. V. Beznoussenko (2009). "Correlative microscopy: a potent tool for the study of rare or unique cellular and tissue events." J Microsc **235**(3): 308-21.
- Newman, G. R. and J. A. Hobot (1999). "Resins for combined light and electron microscopy: a half century of development." Histochem J **31**(8): 495-505.
- Nikonenko, I., B. Boda, S. Alberi and D. Muller (2005). "Application of photoconversion technique for correlated confocal and ultrastructural studies in organotypic slice cultures." Microsc Res Tech **68**(2): 90-6.
- Nisman, R., G. Dellaire, Y. Ren, R. Li and D. P. Bazett-Jones (2004). "Application of quantum dots as probes for correlative fluorescence, conventional, and energy-filtered transmission electron microscopy." J Histochem Cytochem **52**(1): 13-8.

-
- Norgren, R. B., Jr. and M. N. Lehman (1989). "A double-label pre-embedding immunoperoxidase technique for electron microscopy using diaminobenzidine and tetramethylbenzidine as markers." J Histochem Cytochem **37**(8): 1283-9.
- Pathak, R. K. and R. G. Anderson (1989). "Use of dinitrophenol-IgG conjugates to detect sparse antigens by immunogold labeling." J Histochem Cytochem **37**(1): 69-74.
- Pickel, V. M., J. Chan and T. A. Milner (1986). "Autoradiographic detection of [125I]-secondary antiserum: a sensitive light and electron microscopic labeling method compatible with peroxidase immunocytochemistry for dual localization of neuronal antigens." J Histochem Cytochem **34**(6): 707-18.
- Punnonen, E. L., C. Fages, J. Wartiovaara and H. Rauvala (1999). "Ultrastructural localization of beta-actin and amphoterin mRNA in cultured cells: application of tyramide signal amplification and comparison of detection methods." J Histochem Cytochem **47**(1): 99-112.
- Raap, A. K., M. P. van de Corput, R. A. Vervenne, et al. (1995). "Ultra-sensitive FISH using peroxidase-mediated deposition of biotin- or fluorochrome tyramides." Hum Mol Genet **4**(4): 529-34.
- Raimondo, S., M. Fornaro, F. Di Scipio, et al. (2009). "Chapter 5: Methods and protocols in peripheral nerve regeneration experimental research: part II-morphological techniques." Int Rev Neurobiol **87**: 81-103.
- Reynolds, E. S. (1963). "The use of lead citrate at high pH as an electron-opaque stain in electron microscopy." J Cell Biol **17**: 208-12.
- Robinson, J. M., T. Takizawa and D. D. Vandre (2000). "Applications of gold cluster compounds in immunocytochemistry and correlative microscopy: comparison with colloidal gold." J Microsc **199**(Pt 3): 163-79.
- Robinson, J. M. and D. D. Vandre (1997). "Efficient immunocytochemical labeling of leukocyte microtubules with FluoroNanogold: an important tool for correlative microscopy." J Histochem Cytochem **45**(5): 631-42.
- Roth, J. (1996). "The silver anniversary of gold: 25 years of the colloidal gold marker system for immunocytochemistry and histochemistry." Histochem Cell Biol **106**(1): 1-8.
- Roth, J. and M. Binder (1978). "Colloidal gold, ferritin and peroxidase as markers for electron microscopic double labeling lectin techniques." J Histochem Cytochem **26**(3): 163-9.
- Shida, H. and R. Ohga (1990). "Effect of resin use in the post-embedding procedure on immunoelectron microscopy of membranous antigens, with special reference to sensitivity." J Histochem Cytochem **38**(11): 1687-91.
- Silverman, A. J., A. Hou-Yu and B. J. Oldfield (1983). "Ultrastructural identification of noradrenergic nerve terminals and vasopressin-containing neurons of the paraventricular nucleus in the same thin section." J Histochem Cytochem **31**(9): 1151-6.

-
- Singleton, C. D. and V. A. Casagrande (1996). "A reliable and sensitive method for fluorescent photoconversion." J Neurosci Methods **64**(1): 47-54.
- Smiley, J. F. and P. S. Goldman-Rakic (1993). "Silver-enhanced diaminobenzidine-sulfide (SEDS): a technique for high-resolution immunoelectron microscopy demonstrated with monoamine immunoreactivity in monkey cerebral cortex and caudate." J Histochem Cytochem **41**(9): 1393-404.
- Speel, E. J., F. C. Ramaekers and A. H. Hopman (1997). "Sensitive multicolor fluorescence in situ hybridization using catalyzed reporter deposition (CARD) amplification." J Histochem Cytochem **45**(10): 1439-46.
- Stanarius, A., H. Faber-Zuschratter, I. Topel, S. Schulz and G. Wolf (1999). "Tyramide signal amplification in brain immunocytochemistry: adaptation to electron microscopy." J Neurosci Methods **88**(1): 55-61.
- Stierhof, Y. D., H. Schwarz and H. Frank (1986). "Transverse sectioning of plastic-embedded immunolabeled cryosections: morphology and permeability to protein A-colloidal gold complexes." J Ultrastruct Mol Struct Res **97**(1-3): 187-96.
- Takizawa, T., K. Suzuki and J. M. Robinson (1998). "Correlative microscopy using FluoroNanogold on ultrathin cryosections. Proof of principle." J Histochem Cytochem **46**(10): 1097-102.
- Toni, N., E. M. Teng, E. A. Bushong, et al. (2007). "Synapse formation on neurons born in the adult hippocampus." Nat Neurosci **10**(6): 727-34.
- van den Pol, A. N. (1985). "Silver-intensified gold and peroxidase as dual ultrastructural immunolabels for pre- and postsynaptic neurotransmitters." Science **228**(4697): 332-5.
- van Gijlswijk, R. P., H. J. Zijlmans, J. Wiegant, et al. (1997). "Fluorochrome-labeled tyramides: use in immunocytochemistry and fluorescence in situ hybridization." J Histochem Cytochem **45**(3): 375-82.
- Webster, P., H. Schwarz and G. Griffiths (2008). "Preparation of cells and tissues for immuno EM." Methods Cell Biol **88**: 45-58.
- Wigle, D. A., N. N. Radakovic, S. L. Venance and S. C. Pang (1993). "Enhanced chemiluminescence with catalyzed reporter deposition for increasing the sensitivity of western blotting." Biotechniques **14**(4): 562-3.
- Zini, N., L. Solimando, C. Cinti and N. M. Maraldi (2004). "Single and double colloidal gold labeling in postembedding immunoelectron microscopy." Methods Mol Biol **285**: 161-9.

9 Danksagung

Für die Betreuung und Anleitung meiner Arbeit am Institut für integrative Neuroanatomie möchte ich mich ganz herzlich bei Prof. Dr. Rüdiger W. Veh bedanken. Sowohl die Bereitstellung des spannenden Forschungsthemas als auch zahlreiche interessante Gespräche und Diskussionen haben mein Interesse an der Wissenschaft geweckt und mein wissenschaftliches Arbeiten nachhaltig geprägt.

Im Besonderen gebührt mein Dank Dr. Gregor Laube, durch dessen Hilfsbereitschaft es mir ermöglicht wurde, die praktischen Hürden der Elektronenmikroskopie und der elektronenmikroskopischen Immunocytochemie zu meistern. Seine hilfreichen Anregungen im wissenschaftlichen Diskurs haben zudem maßgeblich zum Gelingen dieser Arbeit beigetragen.

Des Weiteren möchte ich mich bei den zahlreichen wissenschaftlichen und technischen Arbeitskollegen im Institut für integrative Neuroanatomie bedanken, durch deren Hilfe, Kollegialität und Anteilnahme mir so manche schwierige Phase der Laborarbeit erleichtert wurde.

Federico danke ich für unsere inzwischen zwei Jahrzehnte währende aufrichtige Freundschaft.

An letzter Stelle, aber nicht zuletzt geht mein Dank an meine Familie, die mir stets zur Seite steht: Köszönöm szépen!

10 Erklärung

„Ich, Vince István Madai, erkläre, dass ich die vorgelegte Dissertation mit dem Thema:

“Virtual Pre-embedding Labeling”: A Method for Correlative Fluorescence and Electron Microscopic Imaging and Double-Labeling in the Central Nervous System of the Rat”

selbst verfasst und keine anderen als die angegebenen Quellen und Hilfsmittel benutzt, ohne die (unzulässige) Hilfe Dritter verfasst und auch in Teilen keine Kopien anderer Arbeiten dargestellt habe.“

Datum

Unterschrift

11 Lebenslauf und Bibliographie

Der Lebenslauf ist in der Online-Version aus Gründen des Datenschutzes nicht enthalten.

BIBLIOGRAPHIEPublikationen mit "peer review"

Poller WC, Bernard R, Derst C, Weiss T, **Madai VI**, Veh RW. *Lateral habenular neurons projecting to reward-processing monoaminergic nuclei express hyperpolarization-activated nucleotid-gated cation channels*. Neuroscience 2011

Madai VI, Altaner A, Stengl KL, Zaro-Weber O, Heiss WD, von Samson-Himmelstjerna FC, Sobesky J. *Crossed cerebellar diaschisis after stroke: can perfusion-weighted MRI show functional inactivation?*. J Cereb Blood Flow Metab 2011

Brinschwitz K, Dittgen A, **Madai VI**, Lommel R, Geisler S, Veh RW. *Glutamatergic axons from the lateral habenula mainly terminate on GABAergic neurons of the ventral midbrain*. Neuroscience 2010

Eingereichte Publikationen mit "peer review"

Madai VI, Poller WC, Peters D, Berger J, Paliege K, Bernard R, Veh RW, Laube G. *Synaptic localization of agmatinase in rat cerebral cortex revealed by virtual pre-embedding*.

Posterpräsentationen

Madai VI, von Samson-Himmelstjerna FC, Stengl KL, Zaro-Weber O, Sobesky J. *Estimation of Ischemic Lesion Age by MRI: Does DWI have FLAIR?* XXth European Stroke Conference, Hamburg, 24. – 27.05.2011

Madai VI, Stengl KL, Zaro-Weber O, Sobesky J. *Bestimmung des Infarktalters mittels MRT. Hat die DWI auch FLAIR?* ANIM 2011, Leipzig, 12. – 15.01. 2011

Madai VI, Bernard R, Poller WC, Laube G, Veh RW. *Virtual Pre-embedding Labeling: A novel method for correlative microscopy and double labeling in brain tissue sections*. Neuroscience 2010, 40th annual meeting of the Society for Neuroscience, San Diego, CA, USA, 13. – 17.10. 2010

Madai VI, Stengl KL, Zaro-Weber O, Heiss WD, Sobesky J. *Crossed Cerebellar Diaschisis: Ist die Darstellung mittels Kernspintomographie möglich?* Neurowoche 2010, Mannheim, 21. – 25.09.2010